UNIVERSITY OF OULU

FACULTY OF INFORMATION TECHNOLOGY AND ELECTRICAL ENGINEERING

DEGREE PROGRAMME IN ELECTRONICS AND COMMUNICATIONS ENGINEERING

MASTER'S THESIS

Reflection Insertion Loss Measurements of Building Materials from 5 GHz to 170 GHz with Varied Angles

Author	Ali-Akbar Abdali
Supervisor	Marko E Leinonen
Second Examiner	Pekka Kyösti

June 2022

Abdali A-A. (2022) Reflection Insertion Loss Measurements of Building Materials from 5 GHz to 170 GHz with Varied Angles. University of Oulu, Faculty of Information Technology and Electrical Engineering, Degree Programme in Electronics and Communications Engineering. Master's Thesis, 47 p.

ABSTRACT

Wireless systems can be characterized with materials surrounding them. Different materials react uniquely to radio waves. This effect becomes further noticeable in high frequencies. Therefore, reflection properties of these materials are important for designing indoor wireless systems of the future. This work focuses on measuring and studying the reflection quality of five common building materials in the frequency bands of 6 – 50 GHz and 110 – 170 GHz. The former frequency band also covers all possible polarization permutations. For the first measurement set, two dual polarized antennas and a 4 port vector signal analyzer (VNA) were used. The latter measurements required two 110 – 170 GHz linear polarized antennas, frequency extenders and 4 port VNA, as well. Averaging is applied to results to eliminate outliers caused by measurement noise.

The theory part covers antennas and their fundamentals such as radiation pattern and beamwidth. Following the radiation pattern, the antennas were placed at the minimum distance from the material samples to get the far field results. S-parameters is also discussed, which is important for the measurements. The dual polarized measurements use four ports to get both co- and cross-polarizations results. The 110 - 170GHz measurements only need two ports for the measurements, because of one type of polarization.

Key words: angle of incidence, building materials, reflection loss, wideband.

Abdali A-A. (2022) Rakennusmateriaalien heijastuslisäyshäviön mittaukset 5 GHz - 170 GHz vaihtelevilla kulmilla. Oulun yliopisto, tieto- ja sähkötekniikan tiedekunta, elektroniikan ja tietoliikennetekniikan tutkinto-ohjelma. Diplomityö, 47 p.

TIIVISTELMÄ

Langattomat järjestelmät voidaan luonnehtia niitä ympäröivillä materiaaleilla. Eri materiaalit reagoivat yksilöllisesti radioaalloille. Tämä vaikutus tulee entisestään havaittavaksi korkeilla taajuuksilla. Siksi näiden materiaalien heijastusominaisuudet ovat tärkeitä tulevaisuuden langattomien sisäjärjestelmien suunnittelussa. Tämä työ keskittyy viiden yleisen rakennusmateriaalin heijastuslaadun mittaamiseen ja tutkimiseen taajuusalueilla 6 – 50 GHz ja 110 – 170 GHz. Ensimmäinen taajuuskaista kattaa myös kaikki mahdolliset polarisaatiopermutaatiot. Ensimmäisessä mittaussarjassa käytetään kahta kaksoispolarisoitua antennia ja 4-porttista piirikonetta. Jälkimmäisiin mittauksiin käytettiin kahta 110 – 170 GHz lineaaripolarisoitua antennia ja taajuuslaajentimia. Mittaustulosten analysoinnissa käytettiin keskiarvoistusta pienentämään kohinaisten mittaustulosten vaihtelua.

Teoriaosuudessa käsitellään antenneja ja niiden perusteita, kuten säteilykuviota ja keilanleveyttä. Säteilykuvion mukaisesti antennit asetettiin minimietäisyydelle materiaalinäytteistä kaukokentän tulosten saamiseksi. Myös S-parametreja käsitellään, mikä on tärkeää mittausten kannalta. Kaksoispolarisoidut mittaukset käyttävät neljää porttia saman polarisaatio tuloksien ja ristipolarisaatioiden tuloksien saamiseksi. 110 – 170 GHz mittaukset tarvitsevat vain kaksi porttia mittauksiin yhden polarisaation vuoksi.

Avainsanat: heijastushäviö, laajakaista, rakennusmateriaalit, tulokulma.

TABLE OF CONTENTS

FOREWORD

This thesis was carried out at the University of Oulu in the Center for Wireless Communications for completion of my master's degree.

I'd like to thank my supervisors Marko Leinonen and Pekka Kyösti for their support and dedication in helping me finish this thesis. They pushed me constantly forward with their questions, comments and help. I'd also like to thank Klaus Nevala who assisted me greatly with the measurements in the laboratory and Juha-Pekka Mäkelä for his help in building up the measurement setup.

I'd like to thank my parents and siblings in supporting and encouraging me through every step of this arduous journey.

Oulu, June 22 2022

Ali-Akbar Abdali

LIST OF ABBREVIATIONS AND SYMBOLS

Γ	input power reflection coefficient
λ	wavelength
a	incident wave
b	reflected wave
D	largest dimension of the antenna
D	directivity
G	gain
k	efficiency
m^2	square meter
P_{refl}	reflected power
P_{inc}	incident power
R	distance
S	scattering
s_{11}	input reflection coefficient
s_{12}	output reflection coefficient
s_{21}	forward transmission coefficient
s_{22}	reverse transmission coefficient
W	power
Z_{ant}	input impedance of the antenna
Z_c	characteristic impedance of the transmission line
CW	continuous wave
DUT	device under test
ECAL	electronic calibration
E	electric field
EM	electromagnetic
EMC	anechoic chamber
FNBW	first null beam width
H	magnetic field
HPBW	half power beam width
IF	intermediate frequency
LHCP	left-hand-circular polarization
LO	local oscillator
LOS	line of sight
RCHP	right-hand-circular polarization
RF	radio frequency
SWR	standing wave ratio
UHF	ultra high frequency
VDI	Virginia Diodes Inc.
VNA	vector network analyzer
VNAX	vector network analyzer extender module
VSWR	voltage standing wave ratio

1 INTRODUCTION

Over half of mobile communications use is indoors and the percentage might even increase to 90% in the next few years according to some analysists. Whether it be someone's home, in the office or public building. Conventional architecture is reaching its limits in providing reliable indoor service for modern users. Volume of mobile data and customers' expectations for a minimum data rate are increasing. Modern phones' support of wide range of frequency bands in small-form factors reduces sensitivity and have to be compensated with increasing signal strength. These frequency bands at over 1 GHz experience greater losses than lower frequency bands. Wanting to increase the thermal insulation of buildings also leads to greater use of denser and more conductive external construction materials. [1]

Clutter and objects surrounding transmitters and receivers in a wireless system especially characterize mobile propagation channels. Indoor scenarios being more densely populated with obstructions have stronger effect in deciding the way the signal propagates along a specific path. These can be walls, clutter and partitions of different materials and open spaces such as doors and atriums. Therefore, it is very important to record the characteristics of different indoor materials in order to understand changes and variations in field strength. Reflections and scattering depend on the material's shape and roughness which in turn affects the amount of loss upon the radio wave impinging onto them. [1]

The reflection properties of this work's materials were measured in a free-space area with a four-port vector network analyzer (VNA) for 6 – 50 GHz frequency band and a four-port VNA with frequency extenders for the 110 – 170 GHz frequency band. The four port VNA allows for the measurement of all the possible co- and cross-polarization reflection results at the same time with dual polarized antennas. Coaxial cables were used to connect the antennas to the VNAs and the higher frequency band also required frequency extenders. The angles measured were from 10 degrees to 80 degrees, except for 70 degrees maximum for the sidewall sample, with steps of five. Unwanted noise was reduced as much as possible by calibrating the set with either an electronic calibration (ECAL) kit or by the VNA itself. High frequency absorption blocks were placed between the antennas so that the antennas picked up mostly the waves reflecting from the material. The results were smoothed in Matlab additionally and portrayed as a 3-D contour plot, where the x-axis is the frequency, y-axis is the angle of antennas, and the magnitude of the reflection is shown inside the graph. The figures of each material resembled each other well enough to ensure consistency. The figures were studied and commented on.

2 THEORY

Antennas has significant importance in communication systems because of their ability for proper transmission and reception of electromagnetic waves. The design of the antenna need to be done based on system requirements in communication links. The antenna design influences the complexity of hardware implementation and impact the overall system performance. Antennas come in variety of shapes and sizes and choosing an antenna for a specific application (cellular, ground-based, cellular-based, etc.) comes down on the following details: the nature of the application (video, audio, data, etc), platform of choice (building, car, ship, etc.), the environment (land, sea, space, etc.) and the frequency of operation. [2]

Electrical signals have two ways to be carried between points, via transmission line or through empty space with the help of antennas at the terminals. Transmission lines encloses the electrical signals and the associated electromagnetic waves' energy near the region or inside the transmission line. Antennas do the opposite. They encourage the electrical signals to reach large distances further from the antenna, which is to radiate. By IEEE definition, they are "that part of a transmitting or receiving system that is designated to radiate or to receive electromagnetic waves". Antennas require no guiding structure, while transmission lines need at least one guiding structure such as a conductor generally. Antenna can then be seen as a transducer that either converts a guided wave from a transmission line to a free-space electromagnetic wave for transmitting case, or the opposite for receiving case. Antennas by large are reciprocal devices and exhibit same behaviour in both transmit and receive modes. They are treated as either one depending on the situation. [3]

All antennas have directional characteristics which is to say that the electromagnetic power density radiates with varying intensity around the transmitting antenna [3]. The ideal antenna for most scenarios radiates all the power fed to it in the wanted direction or directions with the wanted polarization. It is impossible to do so for practical antennas, but their performance can be described. Principal parameters of antennas are radiation pattern, radiation efficiency, the input impedance and bandwidth. Rest of the parameters can be categorized under these groups such as the gain, beamwidth, beam polarization and radiation efficiency. [4]

2.1 Antenna Fundamentals

2.1.1 Radiation Pattern

Radiation pattern is defined as the spatial distribution of a quantity that characterizes the electromagnetic field produced by an antenna. With distance R, the field intensity of the propagating wave decreases by $1/R$. For explaining radiation, let's consider a pulse of electric charge traveling on a straight conductor. Radiation does not happen when the electric charge either static or moving with a uniform velocity. Radiation only happens when the charge is accelerated along the conductor and decelerated having reflected from the end. Thus, radiation fields are generated along the conductor and at both ends. [2]

The space around an antenna is separated radially into three regions. The first is the reactive near-field region which is just a portion of the overall near region immediately surrounding the antenna. In this region, the reactive field dominates. The middle region is known as the radiating near-field region or Fresnel region and covers the rest of the overall near-field region. Here, the angular field distribution depends on the distance from the antenna. The third region is the far-field region or Fraunhofer region, where the angular field distribution isn't dependent on the

distance from a specified point in the antenna region. [2] Equation 1 shows the extend of reactive near-field, equation 2 the extends of the radiating near-field and equation 3 the minimum distance for the Fraunhofer region [5]

$$R_1 < 0.62\sqrt{D^2/\lambda}, \tag{1}$$

$$0.62\sqrt{D^3/\lambda} < R_2 < 2D^2/\lambda, \tag{2}$$

$$R_3 > 2D^2/\lambda, \tag{3}$$

where D is the largest dimension of the antenna and λ is the wavelength. The Fraunhofer region extends after that minimum distance to infinity. There far field observations can be made. [2] Pattern, gain, directivity, and polarization parameters of an antenna are essentially far-field terms because they take advantage of the simplicity of far-field. They do not have to take into account the complexities of reactive near-field [4]. Different antenna radiation regions are shown in Figure 1.

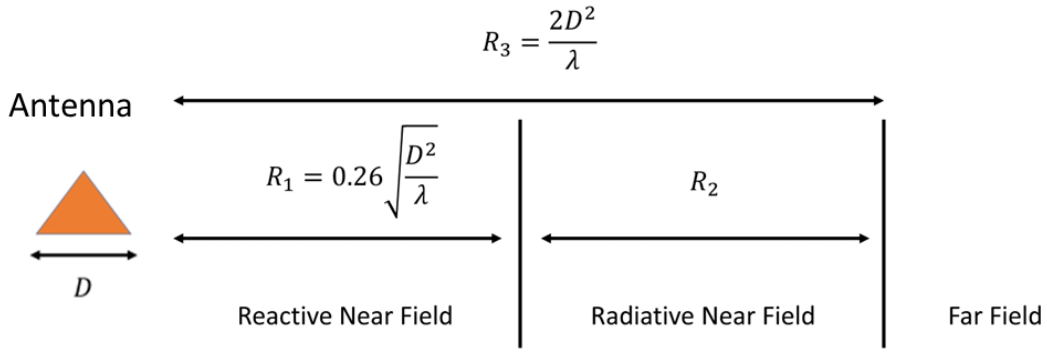

Figure 1. The radiation regions.

2.1.2 Antenna Directivity and Gain

Antenna is basically a spatial amplifier, and directivity compares how much greater the peak radiation level of an antenna is to an antenna with uniformly distributed radiation power. A lossless antenna that radiates uniformly to all directions is known as an isotrope radiator. Practical antennas show nonuniformity of some kind in their patterns. An isotrope and a directional antenna both radiates same amount of radio frequency (RF) power, but the latter sends more power to some directions and less power to compensate to other directions [4]. Directivity can either be interpretated as a ratio of maximum to average radiation intensities, which are dimensionless, or ratio of maximum power to average power densities, which have units of W/m^2, power per square meters. Directivity is entirely affected by the pattern shape and is independent of the details of antenna hardware. [3]

A gain of an antenna is a ratio of the radiation intensity in a given direction to the radiation intensity that would be obtained if the power accepted by the antenna were radiated isotropically. Thus, the gain is therefore obtained from radiation intensity comparison between the studied antenna and the isotrope antanna with the same input power. Actual antenna is also affected by its power being dissipated in ohmic resistance (i.e. converted to heat) whereas an

isotrope is ideally lossless. Gain therefore takes into account the efficiency of the antenna in addition to its directional properties. This relationship can be seen in equation 4

$$G = kD, \tag{4}$$

where G is the gain, k is the efficiency and D is the directivity. [4] Concluding from the equation, a perfectly matched antenna would have equal gain and directivity. The efficiency k includes losses due to mismatch at the antenna terminals and dielectric and conduction losses [2].

2.1.3 Antenna Beamwidth

An antenna beamwidth is the angular width of a single major "lobe" of the antenna that most of the radiated power has concentrated into. Only antennas of this type would the term beamwidth be used with. For example, the radiation pattern of some antennas would have multiple lobes with roughly the same maximum power density, or gain, although not possibly all of the same angular width. Beamwidth wouldn't apply for these antennas. [4]

There are multiple definitions for the beamwidth of the antenna. One definition is to cite the width of the beam between the two nulls (zero-values) on both ends of the maximum which is called first null beamwidth (FNBW). Although common, not all beams have such nulls. It is also more logical for the beamwidth to indicate the angular range, where radiation of useful strength is, or over which good reception may be anticipated. This has led to the the adopted convention of the second definition to measure beamwidth where the start and end are the points with power densities half of the maximum. This definition is called half power beamwidth (HPBW). These points correspond to minus 3 dB points with ordinate scale in decibels. Thus, half-power beamwidth is also called as the 3 dB beamwidth. [4]

2.1.4 Impedance Matching

Antennas are associated with two types of impedances: a self and a mutual impedance. Self-impedance is the driving-point impedance, when the antenna radiates into unbounded medium with it not coupled to other antennas or surrounding objects. The driving point impedance becomes a function of its self-impedance and the mutual impedances with other sources and objects, when there is coupling between the antenna under test and other sources or objects. This driving point impedance is known as the input impedance practically. [6]

For maximum power transfer, a conjugate match between a source or a source-transmission line and an antenna is wanted. If the system is mismatched, some of the incident or available power is reflected at the input terminals into the line. Constructive and destructive interference patterns are created from the combination of the reflected waves and the traveling waves from the source to the antenna. These standing waves amount to pockets of energy concentrations and storage inside the transmission line like resonant devices. What determines the amount of power to be reflected is the degree of mismatch which is a function of the input impedance of the antenna and the characteristic impedance of the line. Equation 5 shows the standard transmission-line relationship which relates the impedances with input voltage reflection coefficient Γ and the input voltage standing wave ratio VSWR.

$$\frac{P_{refl}}{P_{inc}} = |\Gamma|^2 = \frac{|Z_{ant} - Z_c|^2}{|Z_{ant} + Z_c|^2} = \frac{|VSWR - 1|^2}{|VSWR + 1|}, \quad (5)$$

where P_{refl} is the reflected power, P_{inc} is the incident power, Z_{ant} is the input impedance of the antenna and Z_c characteristic impedance of the transmission line. Equation 6 shows the individual voltage reflection coefficient being ratio of reflected voltage and traveling voltage

$$\Gamma = \frac{Z_{ant} - Z_c}{Z_{ant} + Z_c}, \quad (6)$$

and equation 7 shows the individual VSWR being the function of voltage reflection coefficient

$$VSWR = |\Gamma|^2 = \frac{1 + |\Gamma|}{1 - |\Gamma|}. \quad (7)$$

In an impedance matched system, the VSWR is 1 and Γ is 0 [6].

2.2 Wave Propagation

There are three basic propagation mechanisms: reflection, diffraction and scattering. This work focuses especially on the reflection and scattering properties of different materials at varying frequencies. [7]

Reflection describes a situation where the propagating signal touches an object with large proportions compared to the wavelength of the signal. Then, the object surface seems smooth to the wave. It can occur from walls and windows to even multitudes larger objects like planets.

Diffraction happens when the object's surface has edges which lead to secondary waves being present around the space and on the other side of the obstacle. So, even when there is not an established line-of-sight, waves can be bending throughout the obstacle. [7]

Lastly, there is scattering. opposite of reflection, the medium is made up of multiple objects of smaller dimensions than the propagating wavelength. Simply, rougher edges and smaller objects cause scattering. Practically, common outdoor environment can cause scattering such as foliage and street signs. [7]

Both reflection and diffraction are affected by geometry of the object and amplitude at high frequencies. Also affecting are amplitude, phase, and polarization of the incident wave at the point of diffraction. Surface of most indoor objects are treated as smooth at lower frequencies. Increasing frequency causes the wavelength to eventually get so short that even seemingly smooth surfaces reveal their roughness. Therefore, reflection can turn into scattering. [7]

Figure 2 shows how a radio wave would behave in each scenario.

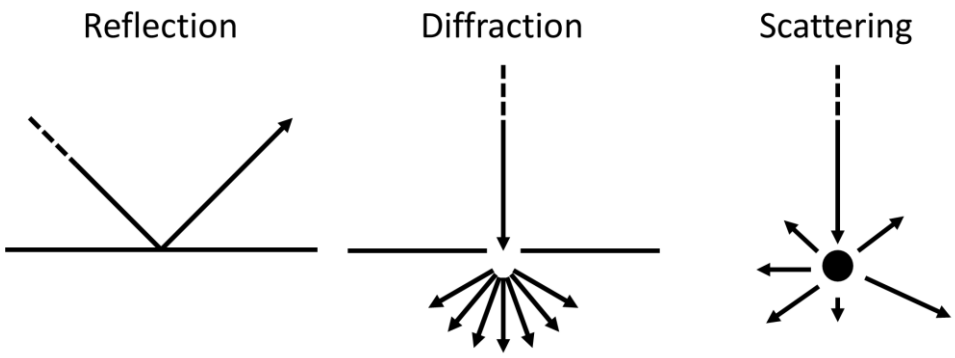

Figure 2. The three propagation mechanisms.

2.3 Polarization

Both electric fields and magnetic fields exist in electromagnetic (EM) waves which are related through Maxwell's equations. Maxwell's equations describe the dynamic behaviour of these fields such that a time varying electric field has to be accompanied by a time varying magnetic field. In free-space propagation where there is no confinement, the wave results into traveling-motion wave and spreads farther from the source. Then, the wave becomes a plane wave in which the electric fields and magnetic fields are perpendicular to each other in addition to the wave direction. The phase of these fields are equal over a plane also perpendicular to the propagation direction. Polarization can then be expressed by the time variations of the of the electric field vector. [8]

Polarization of an antenna refers to the polarization of the wave resulting from the radiation the antenna transmits in the given direction. The polarization would be the local plane wave at points on a radiation sphere centred on the antenna. Polarization of the antenna is therefore determined by observing the wave polarization from a transmitting antenna at various angles in the far field. Polarization typically changes with angle, so polarization is commonly stated in the direction of the main beam peak. Dual-polarized antennas are unique in the sense that they can produce either intended polarization, co-polarization, or cross polarization. [8]

Co-polarization is when both of the polarizations of the components are the same. Cross-polarization is orthogonal state of co-polarized wave. Cross-polarization is unwanted because it results from self-interference and cross-talk between two signal channels. Real antennas are never perfectly orthogonal, but they are stated as such orthogonal if they are nearly so [8]. Depending on the polarization of both the incoming wave and of the receiving antenna, the available power changes. Polarization mismatch can be described as a loss in the sense that less power is available from the wave when the antenna is mismatched polarization wise compared to when it is matched. Examples of cross-polarized states are orthogonal linear states (horizontal, vertical) and right- and left-hand circular polarizations [3].

Figure 3 shows a plane wave in free space.

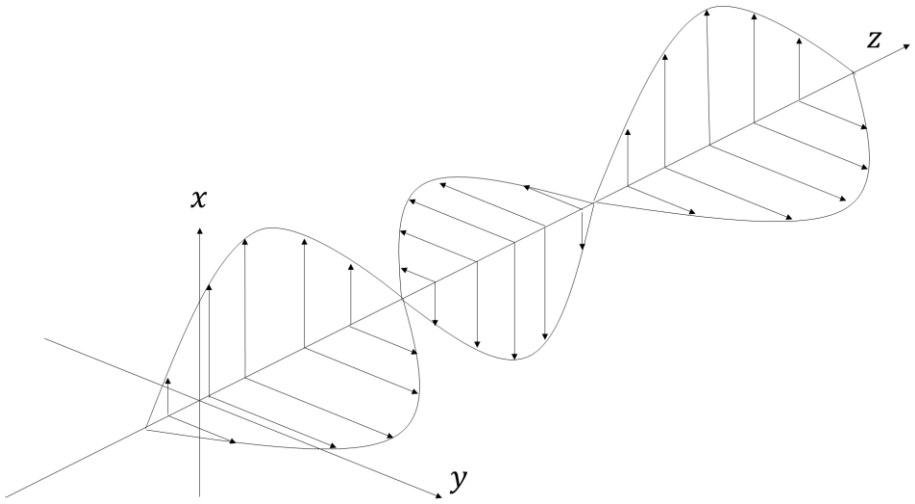

Figure 3. Plane electromagnetic wave in free space.

2.3.1 Linear Polarization

Plane wave is a linearly polarized when the electric field vector has a particular direction in space for all values of z. The plane wave is linearly polarized in the x-direction in figure 1. In actual space above earth, wave is either vertically or horizontally polarized. Vertical polarization happens when the electric vector is vertical or is laid out on vertical plane. If the electric vector is horizontal or lays on the horizontal plane, its polarization is horizontal. [4]

2.3.2 Circular Polarization

Circular polarization appears to be rotating around the z-axis from the viewpoint of a fixed observer. It makes one full turn for each cycle. This rotation can be either going clockwise or counter clockwise. The former corresponds with right-hand-circular polarization (RHCP) and the latter with left-hand-circular polarization (LHCP). Circular polarization is the combination of two linearly polarized waves. They have to be launched simultaneously and in the same direction. Additional caveats are that they have to be at right angles to each other and their phase angles. This means that the initial phase angle between the electric field and magnetic field differ by $\pi/2$ (90 degrees). If the phase difference is positive, it is rotating clockwise. Negative phase difference leads to counter clockwise rotation. [4]

The handedness of the polarization comes from the right-hand rule. The thumb of the hand is pointed towards the direction of propagation and the fingers will then curl in the direction of the electric field rotation. Whichever hand suits the direction of the electric field rotation, the circular polarization is that handed. Some presentations might use the direction of travel toward the observer in which case the clockwise rotation corresponds to LHCP and counter clockwise rotation to RHCP. This is not needed for linear polarization, because it is basically an elliptical polarization with the ellipse collapsed into a line. In this special case, the rotation is meaningless. [8]

2.3.3 Elliptical Polarization

Circular polarization can also be seen as a special case of elliptical polarization. A true circular polarization requires for the magnitudes of the two linearly polarized waves to be equal, otherwise, the polarization is elliptical. [4] It is named for the shape that can be observed when tracing the path of the tip of the electric field vector in this case [2]

2.4 Scattering Parameters

Two-port networks have forward and reverse transmissions besides the reflections. VNA characterizes these with scattering parameters (S-parameters) for devices. They are an extremely accurate method in describing the linear behaviour of the component under test [9]. A two-port device with its wave quantities is shown in figure 4.

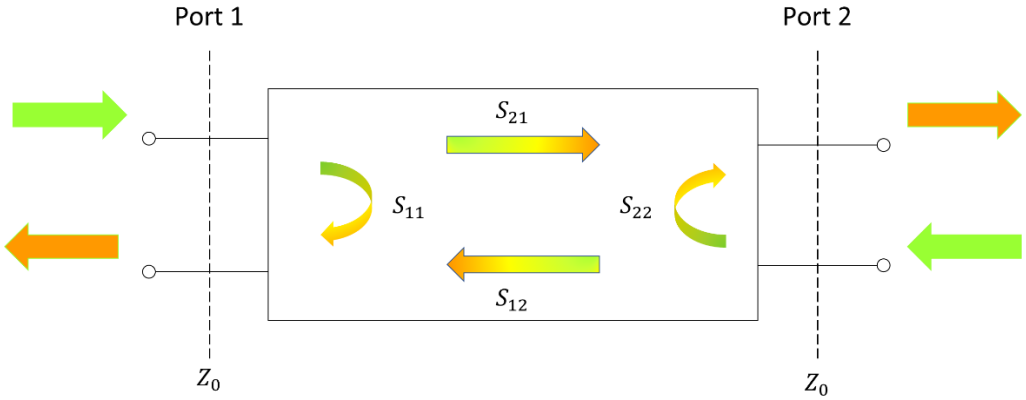

Figure 4. Two-port device with wave quantities.

Power waves going towards ports are defined as $a = (a_1, a_2, \dots, a_n)$ and the waves moving away from the ports are defined as $b = (b_1, b_2, \dots, b_n)$. Therefore, currents going towards the network are marked positively and currents going away are marked negative [10]. Forward transmission measurements use reflectionfree termination $\Gamma = 0$ (match) on port two. While port 1 is powered by the incident wave $a_1 \neq 0$, port 2 stays at zero, $a_2 = 0$. Then, the input reflection coefficient s_{11} can be measured on port 1 (equation 8), and the forward transmission coefficient s_{12} can be measured between ports 1 and 2 (equation 9). [11]

$$s_{11} = \left.\frac{b_1}{a_1}\right|_{a_2=0} \tag{8}$$

$$s_{21} = \left.\frac{b_2}{a_1}\right|_{a_2=0} \tag{9}$$

Likewise in reverse transmission measurements, the match $\Gamma = 0$ is applied to port 1. Port 2 of the network is the one being simulated now by the incident wave $a_2 \neq 0$. Now the output reflection coefficient is measured on port 1 (equation 10), and reverse transmission coefficient between ports 2 and 1 (equation 11).

$$s_{12} = \left.\frac{b_1}{a_2}\right|_{a_1=0} \tag{10}$$

$$s_{22} = \left.\frac{b_2}{a_2}\right|_{a_1=0} \tag{11}$$

Generally, both incident waves can be non-zero, which is then a superposition of the two measurement situations. This is defined in the equations of 12 and 13.

$$b_1 = s_{11}a_1 + s_{12}a_2 \tag{12}$$

$$b_2 = s_{21}a_1 + s_{22}a_2 \tag{13}$$

Grouping the S-parameters together leads to an S-parameter matrix (S-matrix) with wave quantities to obtain the vectors a and b. Equations show this new compact form in the equations of 14 and 15.

$$\begin{bmatrix} b_1 \\ b_2 \end{bmatrix} = \begin{bmatrix} s_{11} & s_{12} \\ s_{21} & s_{22} \end{bmatrix} \begin{bmatrix} a_1 \\ a_2 \end{bmatrix} \tag{14}$$

$$b = Sa \tag{15}$$

One or two port networks are enough to represent many standard components but increasing integration has made devices under test (DUT) with three or more ports more ordinary. Thus, the term N-port has been coined. This work uses both 2- and 4-port networks [11].

3 REFLECTION MEASUREMENTS

The reflection measurements are done based on VNA S-parameter measurements. In such measurement, the test signal is transmitted from the first test port of VNA to the transmission antenna and the reflected test signal from the object under test to other is convoyed to second test port of VNA via reception antenna.

3.1 Vector Network Analyzer

Network analysis is a common and important parts of RF engineering. The networks can range from passive electrical objects such as amplifiers and filters to complex objects used in satellite communications. The impedance measurement can be done by relatively simple tools at lower frequencies: sine wave generator. meters and a calculator. Then Ohm's law can be used to calculate the impedance with the gathered voltage and current data. This has to be repeated individually for all frequencies of interest. At higher frequencies, the complexities increase, and VNAs are needed. VNAs are versatile machines with complex architectures. Necessary tools required in lower frequency measurements are built into them such as meters and calculators. They are designed primarily for measuring incident and reflected waves with great efficiency and accuracy. [9] [12]

The network analyzer generates a sine signal to feed the DUT. Once the signal has returned from the DUT, it has a different amplitude and phase compared to the signal that was fed. The instrument measures the response's impedance and reflection factor. The wave quantities from the signal are therefore used to characterize the DUT. Scalar network analyzers. related to VNAs, only measures the amplitude difference between incident and reflected waves. VNAs go further measuring both wave's amplitude and phase. VNA data can also be transformed from frequency domain to time domain. [12]

3.2 Measurement Setup for 6 – 50 GHz Measurements

The 6 – 50 GHz reflection measurements were done in the radio anechoic chamber (EMC) of the University of Oulu. The measurement setup consists of two antennas, VNA, 2 pairs of coaxial cables of different length, two wooden stands and a wooden half-circle. The used VNA was a 4-port model of N5247A (PNA-X) from Keysight Inc. It has sufficient frequency range to suit the measurements. The coaxial cables are used to connect the antennas and the VNA together. Both measurement antennas 5 to 50 GHz were dual polarized antennas, positioned to vertical and horizontal directions. The setup is illustrated with a block diagram in figure 5.

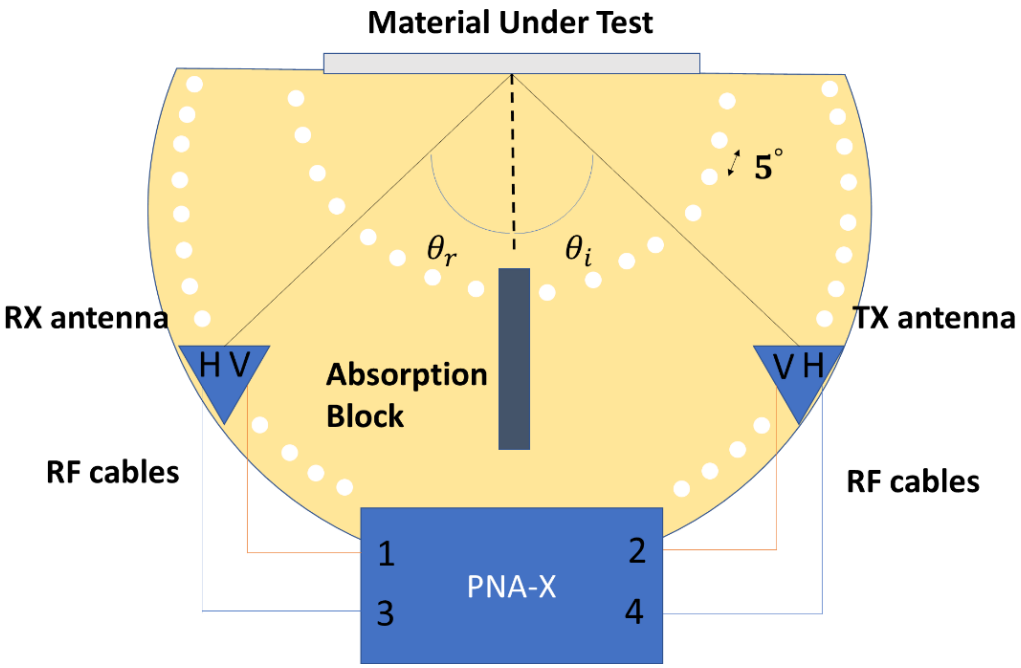

Figure 5. Set-up block diagram of the 6 – 50 GHz measurements.

The reflection measurement setup is a bistatic. The angle at which the antennas are from the centre are the same. To change measurement angles easily and fixed manner, a half circle was made with holes to match 5 degrees of separation each other. The wooden stands slide over piece of wood which are attached to the half circle. These wooden stands can then be adjusted to the wanted distance by sliding them back and forth the board. The measurement antennas are placed at 1.35 meters height on the stand to avoid as much possible reflections from the ground surface or the floor of the EMC chamber. A plastic holder was designed, and 3-D printed to fix the locations of the measurement antennas on the wooden stands. The half circle can have some small angle error, because of its hand handmade quality. The photograph of the measurement system is shown in Figure 6.

For most accurate reflection measurements, frequency absorbing materials were used between the antennas. The absorber prevents a direct test signal leakage from TX to RX antenna and thus the measurement focuses on the reflections, only. The absorbers were placed individually for each angle. At larger angles, this meant that the absorber was placed very close to the sample material. The lower the angle measurement, the absorber was placed more away from the sample.

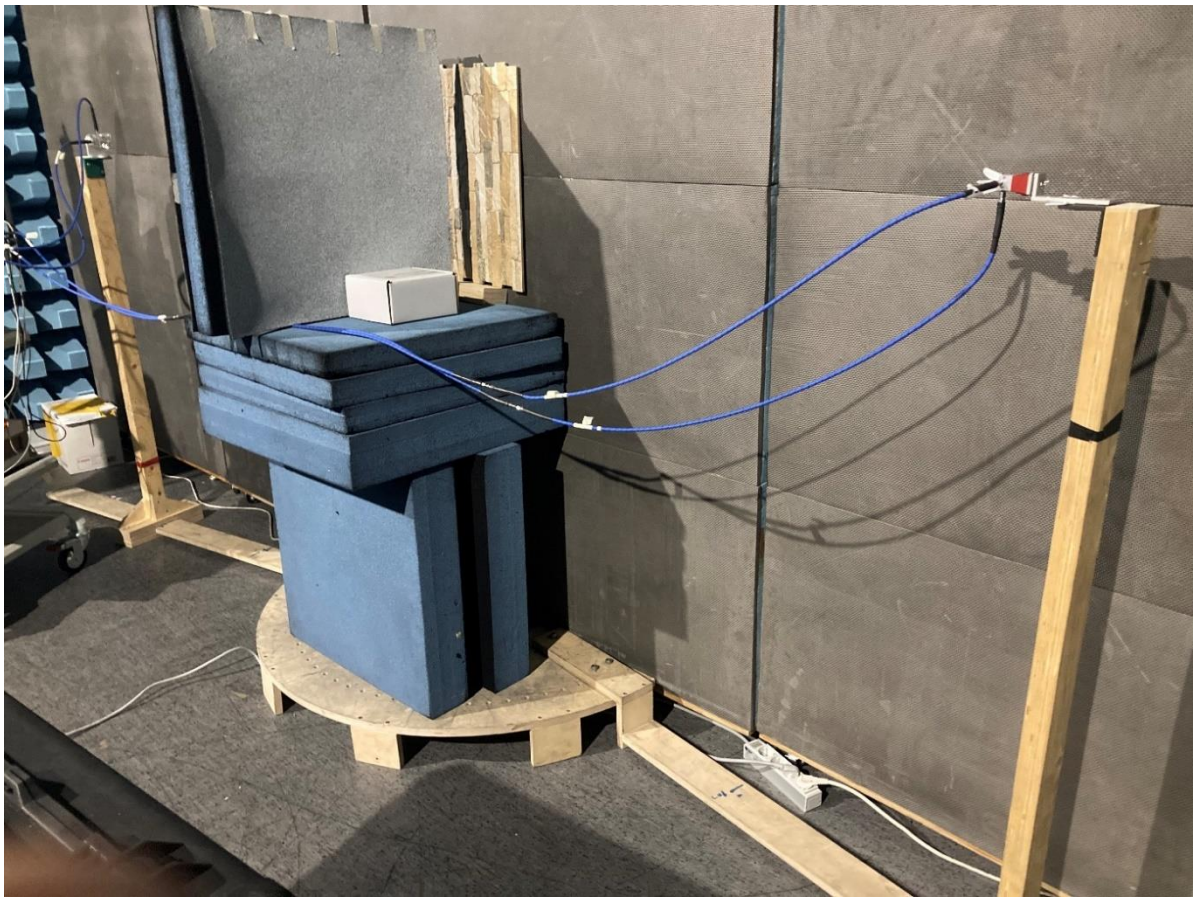

Figure 6. Photograph of dual-polarized 6 – 50 GHz measurement at wide angle measurement.

Table 1 shows the parameters of the VNA and the setup. The VNA was allowed to run at its whole frequency range and then at the data processing part, only the data at the relevant frequencies were used. The calibration was done for 10 MHz to 67 GHz but measurement used subset of the data; 4401 points.

Table 1. Refection measurement setup settings for 6 to 50 GHz frequencies.

Parameter	**Value**
VNA output power	-10 dBm
Number of points	6401
Measurement frequency range	0.01 – 67 GHz
Antenna heights from ground	135 cm
Antenna distances from samples	14 5cm

3.3 Measurement Setup for 110 – 170 GHz Measurements

All the measurements for the 110 – 170 GHz frequency range were also done in the radio anechoic chamber of University of Oulu. The measurement setup involves many of the same equipment as previous 6 – 50 GHz measurements. Different version of the VNA was used which was a 4-port model of N5242B (PNA-X) from Keysight Inc. The horn waveguide

antennas were screwed directly to the frequency extenders. The block diagram of the measurement set-up for 110 to 170 GHz is illustrated in figure 7.

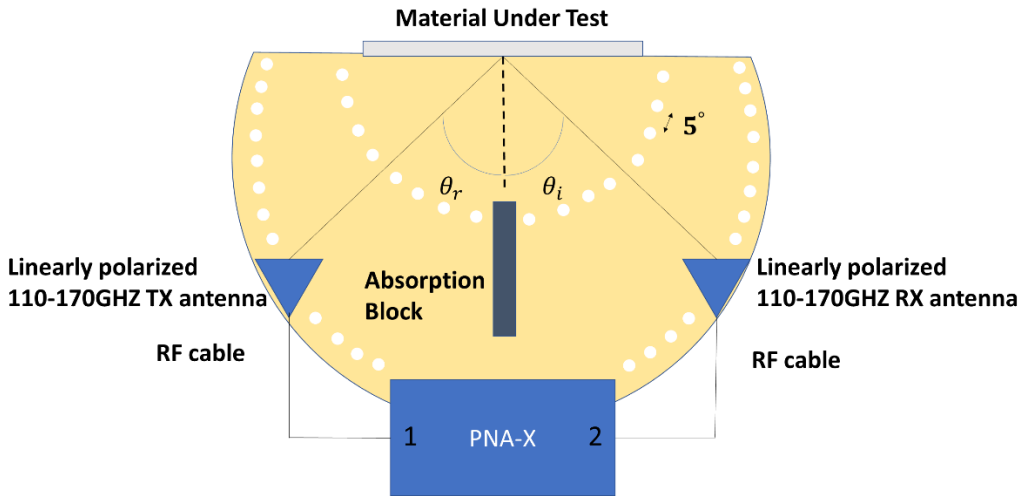

Figure 7. Setup of the 110 – 170 GHz measurements.

The same wooden half-circle and stands were used as in 5 to 50 GHz measurements. The length at which the antennas were setup is the same, as well in the other frequency band measurement. The measurement was faster on higher frequency band since we only measured the reflections in one (horizontal) polarization. The photograph of the 110 to 170 GHz measurement set-up is shown in Figure 8.

Figure 8. 110 – 170 GHz measurement at narrow angle.

Table 2 shows the parameters of this set-up and those do not differ much from the table 1 except here the frequency range is exactly what is desired and thus, the full number of data points is used in the data, 6401.

Table 2. Refection measurement setup settings of 110 to 170 GHz frequencies.

Parameter	Value
VNA output power	-12 dBm
Number of points	6401
Measurement frequency range	110 - 170GHz
Antenna heights from ground	135 cm
Antenna distances from samples	145 cm

3.3.1 Frequency Extenders

The frequency extenders are used to extend the RF measurement equipment measurement range over the original maximum frequency. The 110 – 170 GHz measurements were done with a VNA which maximum frequency range was 26.5 GHz. Two different frequency extenders were used: one supporting the transmission and second supporting the reception. These frequency extenders are different from each other from radio implementation point of view.

The frequency extenders are continuous wave (CW) extenders designed to support VNA (VNAX) made by Virginia Diodes Inc. (VDI). The RF block diagrams of the transmitter module is shown in figure 9 and the block diagram of the receiver module is shown in figure 10.

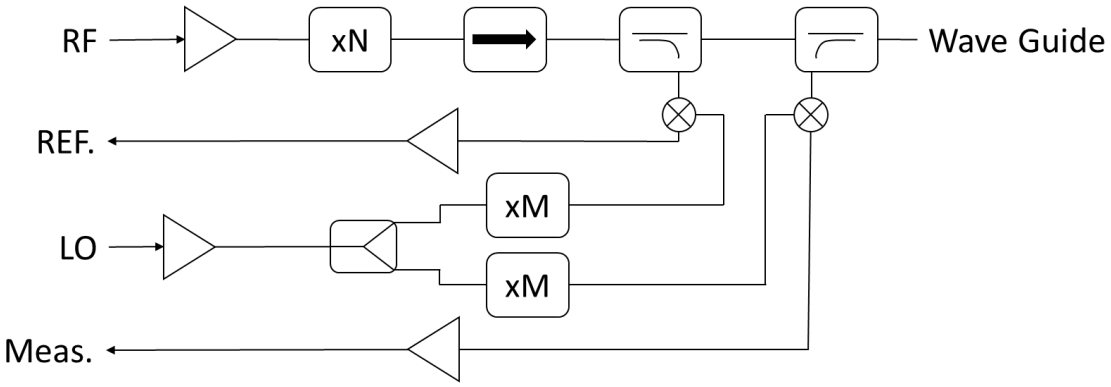

Figure 9. RF block diagram of used extender transmitter module.

The PNA feeds the RF signal to the input port of the VNAX named RF in the figure 5. VNAX has in addition two “back-to-back” directional couplers, connected to each of their own receiver. The first is reference channel receiver or reference mixer to sample the forward wave named REF in the figure 5. The second receiver signal Meas. is appropriately the measurement channel receiver or measurement mixer for the return sample of RF signal. The frequency of the operation is generated by the local oscillator signal named LO in the figure 9. [13]

The two signals that PNA sends, RF and LO and those generate RF test signal following the heterodyne principle. It is essential that the measurement signal’s magnitude and phase information to stay the same. Then the input RF signal at intermediate frequency (IF) is amplified in the output of the extender module named waveguide in the figure 9 Additionally, the RF signal is upconverted to the final RF frequency with LO signal, which is multiplied M times in the LO signal chain. This work’s measurements used two VNAX modules and a one directional 2-port S-parameter measurement can be done. The receiver VNAX module is shown in figure 10. where LO signal is multiplied M times in LO signal chain. This LO signal down-coverts the input signal from waveguide to the IF signal which can be analysed from Meas. port

in figure 10. The receiver frequency extender module is smaller and more lightweight compared with transmission counterpart. [13]

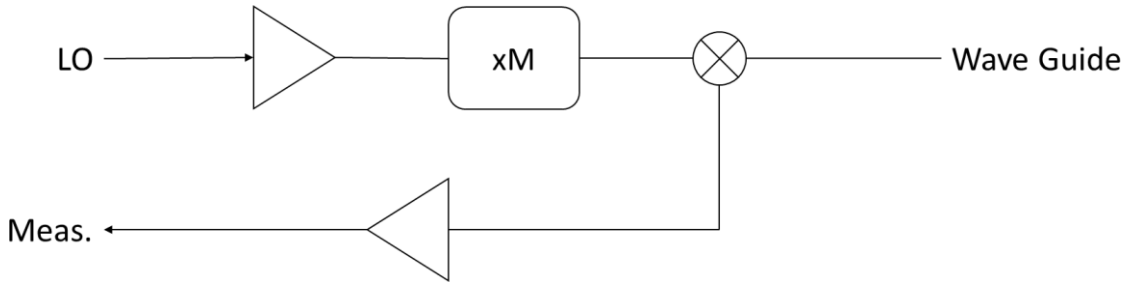

Figure 10. RF block diagram of used extender receiver module.

The exact frequency extender models used for this work are WR6.5-VNAXs. Some main RF specification parameters are listed in table 3 [14].

Table 3. Properties of the used frequency extenders (WR6.5 VNAX by VDI).

Parameter	Value	Unit
Frequency Coverage	110 – 170	GHz
Dynamic range (BW = 10Hz, typical)	120	dB
Dynamic range (BW = 10Hz, minimum)	110	dB
Magnitude stability (±, typical)	0.25	dB
Phase stability (±, typical)	4	degree
Test port power (typ. power)	13	dBm
Directivity (typical)	30	dB

3.3.2 Measurement Antennas

The measurement antennas were standard gain horn antennas. The name comes from their shape with which they radiate radio frequencies from a waveguide out into free space. At the receiver, the radio waves get converted back into a waveguide. Horn antennas are widely used in frequencies above 300 MHz which are ultra high frequencies (UHF) and microwave frequencies and with waveguides [15]. Horn antenna uses its shape to provide an extended aperture to smooth out the otherwise abrupt transformation of a waveguide into radio waves. This maximises the amount of energy radiated and is called flaring. A waveguide terminated by a horn antenna gets impedance matching from the gradual transformation. Being a waveguide fed antenna, it is superior in power handling than other antennas. [16]

Horn antennas come in variety of shapes, each one unique based on their controlling of one or more of antenna fundamental properties. These are gain, radiation pattern and impedance [17]. The three main groups they can be divided into are rectangular, circular and diagonal horn antennas. Rectangular horn antenna can be divided into pyramidal and sectoral antennas depending on the flaring. One other type is the ridged horn antenna, where there are fins built inside the horn. The fins are there to lower the cut-off frequency and as a result, increase the bandwidth. Dual ridged horn antennas have two fins and quad ridged horn antennas have four fins. [16]

The 110 – 170 GHz measurements used the pyramidical horn antennas for both transmitting and receiving. The minimum frequency is 110 GHz and the maximum frequency is 170 GHz. Pyramidal horn antennas are rectangular in shape for cross-section and end. have many

positives. This form has equal radiation patterns in both electric (E) and magnetic (H) fields because it has flaring on both sides. They have high gain and directivity, low standing wave ratio (SWR) and broad bandwidth. [15]

The 6 – 50 GHz measurements uses two different models of dual-polarised antennas. The first antenna's frequency range is 6 – 67 GHz and the second antenna's is 5 – 50 GHz. That leaves the measurement range as 6 – 50 GHz. Both are of the quad ridged horn antenna variety.

Table 4 lists the key parameters of all three antennas: PEWAN1028 [18], LB-SJ-50500 [19] and QRH67E [20]. Using Pythagorean theorem, the diameter of the antenna was calculated as the longest dimensions. Those values were used with equation 1 with their maximum frequency to get the minimum distance from the sample to get the far field results. The longest required distance out of the three was the 5 – 50 GHz quad ridge horn antenna was 1.32 meters.

Table 4. Key parameters of the antennas.

Antenna		**Pewan1028**	**LB-SJ-50500**	**QRH67E**
Type		Pyramidal	Quad ridged	Quad ridged
Frequency range (GHz)		110 - 170	5 – 50	6 - 67
Gain (dBi)		25	12	14
Antenna factor (dB/m)				40 - 54
VSWR (max.)			3.0:1	2.4
VSWR (avg.)		1.15:1	1.5:1	1.4
3dB beamwidth (deg.)	E plane	10	23 to 101 depends on frequency	35 to 105 depends on frequency
	H plane	9	14 to 99 depends on frequency	20 to 110 depends on frequency
Polarization		Linear	Dual linear	Dual linear, circular (with hybrid)
Size (mm)		19.05 x 19.05 x 49.0	44.5 x 44.5 x 77.6	35.1 x 35.1 x 77.5

3.4 Measurement System Calibration

Use of anechoic chamber and radio absorbers helped to reduce external interferences during the measurements. There still persists some uncertainty which needed to be overcome during measurements. The VNA and the frequency extenders need time to warm up. The warm up time of those was 30 minutes that measurement results were stable.

The major uncertainty to the measurements came from the coaxial cables. These can be from rough handling of the cables such as bending and damages from being stepped on. Electrical problems such as impedance mismatches, delays and attenuation are factors which caused problems during measurements. This was further exacerbated with use of different lengths and models of coaxial cables.

For the 5 – 50 GHz measurements, an ECAL kit was used to calibrate all four ports of the VNA. Each port was then tested afterwards to ensure stability. They all performed worst at the higher frequencies, but it was still acceptable enough with the port power used. This calibration process was tedious and connections of the coaxial cables was checked multiple times throughout to avoid any connection loosening. The calibration of the higher frequency setup was much easier and faster. The coaxial cables from port 1 and 2 were connected to transmitter and receiver frequency extenders respectively and the extenders screwed together for a loop. The longer cables were placed in such position that they were straight. The calibration was run

with the help of the VNA alone then. If the VNAs were left on from the previous measurements, they didn't need to be calibrated again.

3.5 Material Samples

All the material samples tested were unique from each other and commonly found in real life. Some of the measured samples are cleaner than the others. The wide range of materials and their quality helps in gathering some observations from the measurements. The materials are also similar in thickness, so that should not factor much in the results. The sizes of the material samples are listed in table 5.

Table 5: Properties of the material samples.

Material	Length (cm)	Height (cm)	Width (cm)
Plywood	90.5	52	0.8
Wood	45.5	32.5	2.5
Plasterboard	90.5	33.5	1.5
Brick	50	33.5	0.7
Sidewall	147	148	3

3.5.1 Plywood

The used plywood sample was no in perfect condition. It had a circle hole in the middle and two smaller ones on the edge. The antennas were pointed so that test signals avoided the circle. Material was not cleaned up and it has the same wear and tear that a real-life wood would have indoors.

This was the most straightforward of the samples to set up since it could be hanged on the wall with a rope it is attached to. The photograph of the sample is shown in figure 11.

Figure 11. Plywood sample.

3.5.2 Wood

The wood sample was made from a cutting board. It had relatively smooth and clean surface. The photograph of the sample is shown in figure 12.

Figure 12. Wood sample.

3.5.3 Plasterboard

The third tested material sample was a piece of plasterboard. It was very flat and uniform on the surface. The photograph of the sample is shown in Figure 13.

Figure 13. Plasterboard sample.

3.5.4 Ceramic Tile

The brick sample was a ceramic tile with a rough surface finishing. Thus, it was a complete opposite material sample compared to the plasterboard surface. The surface area of the tile was ragged and in disarray. The photograph of the sample is shown in Figure 14.

Figure 14. Ceramic tile sample.

3.5.5 Sidewall

The side wall that was measured is similar as office environment's cubicle division wall and photograph is shown in Figure 15. The stand of the material only allowed the maximum angle of 70 degrees compared to other samples' 80 degrees.

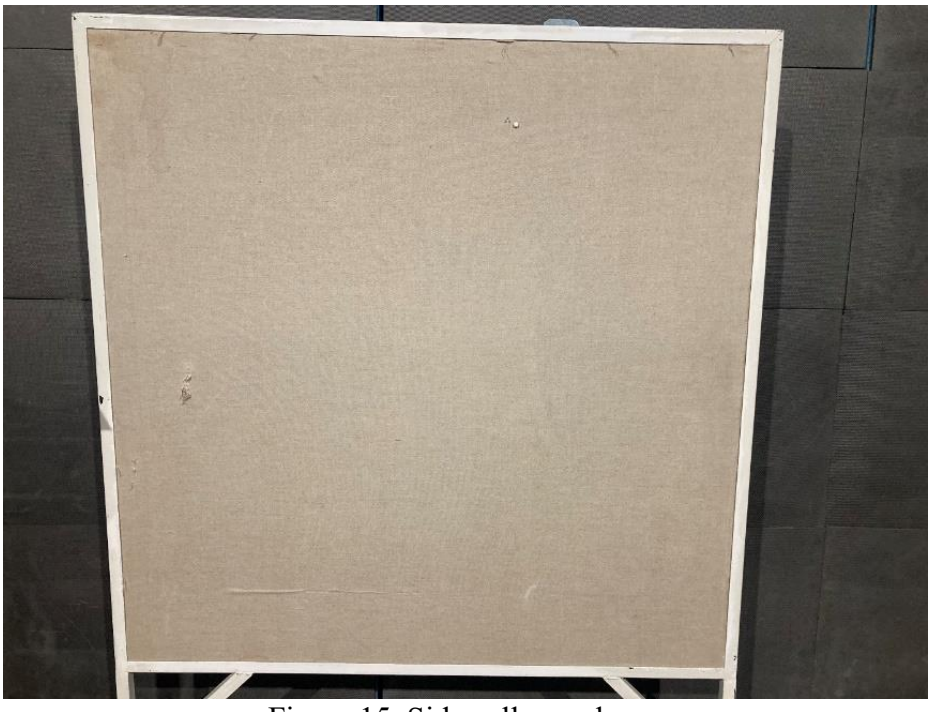

Figure 15. Sidewall sample.

4 MEASUREMENT RESULTS

The data from the measurements were stored on the VNA and transferred through a memory stick. Line of sight (LOS) measurement was performed for both antenna measurement sets, to account for any loss resulting from distance. Some of the results might show positive numbers resulting from the smoothing, but since it was applied to every data, it is still accurate representation.

4.1 6 – 50 GHz Measurements

4.1.1 Plywood

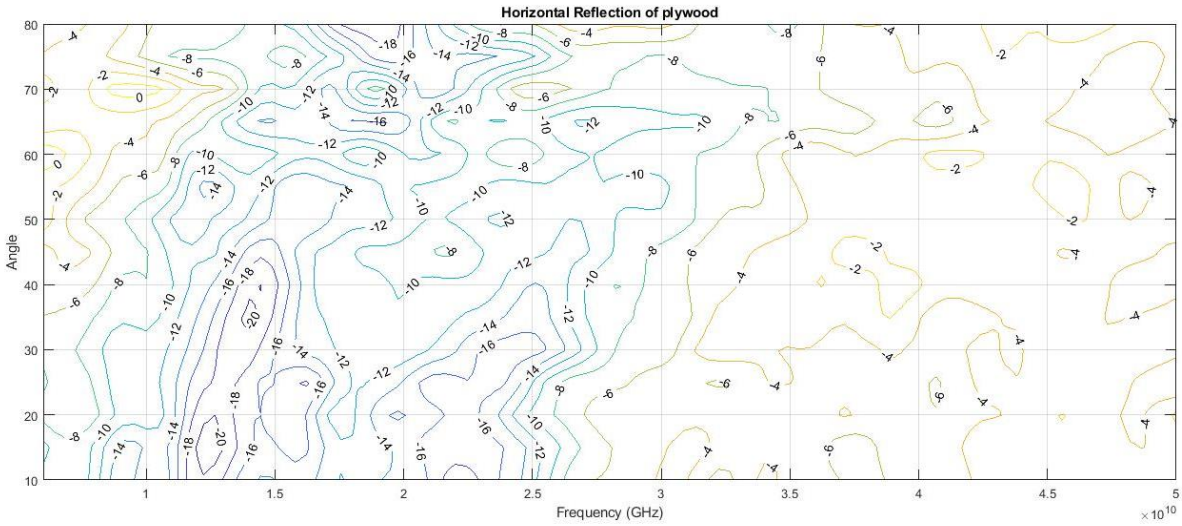

Figure 16. Horizontal polarization of plywood.

The plywood reflects highest reflection attenuation values are between 10 – 30 GHz frequencies in figure 16. At lower frequencies, the attenuation is highest, varying from -10 to -20 dB. Frequencies lower than 1 GHz perform same as frequencies above 3 GHz with results from -6 to -2 dB. This is opposite looking at the angles at y-axis. The reflection losses are smallest at the middle section and degrade the further from the centre in figure 16. This is more noticeable in the lower angles where the antennas are very close to each other, and the angles are sharper. The overall measured reflection loss values varied from -2 to -20 dB.

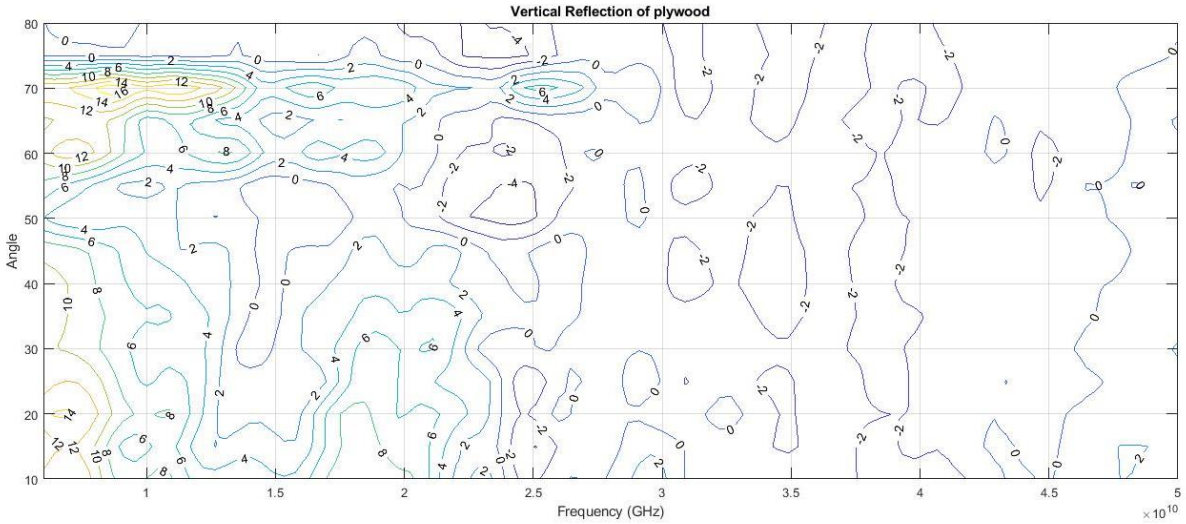

Figure 17. Vertical polarization of plywood.

It can be seen from the vertical results from figure 17 that it is very different to horizontal results in figure 16. Here, there is a noticeable wall happening at 2.5 GHz. The lowest end of the frequencies shows the best results of near 0 dB and it keeps performing worse the higher the frequency scales. As for angle, here too it differs from horizontal with performing best in the outer cases. The worst numbers of -14 dB are still better than most in the horizontal figure.

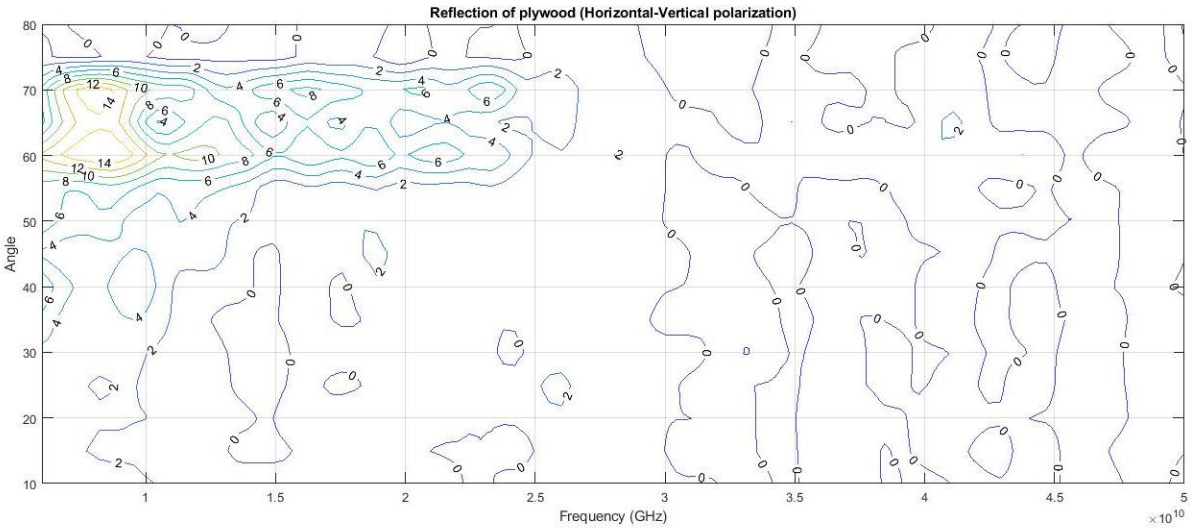

Figure 18. Horizontal-vertical polarization of plywood.

The horizontal-vertical cross-polarization reflection shows surprising results in figure 18. It is only showing the best numbers of up to 14 dB at the roughly 60 - 70 degrees angles. This too performs best in the lowest frequencies, stays the same from 1 GHz to 2.4 GHz where it then looks the same as the rest of the results, full of near 0 dB results. It should be mentioned that it still looks better than horizontal reflections. The figure 18 follows the style of the vertical polarization as shown in figure 17.

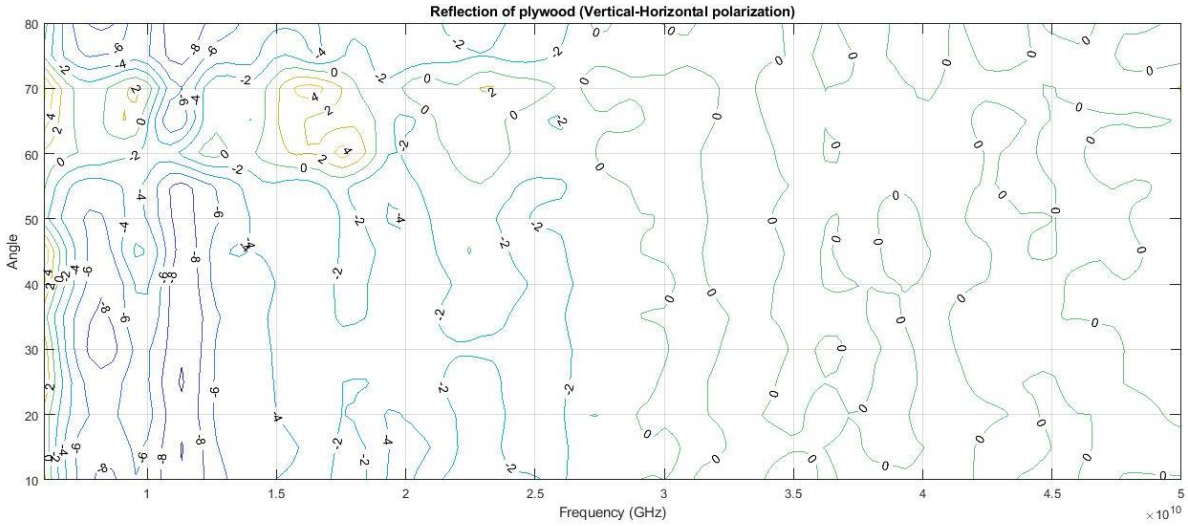

Figure 19. Vertical-horizontal polarization of plywood.

The vertical-horizontal cross-polarization reflection looks to be more influenced by the horizontal reflections than vertical in figure 19. The shift at 2 GHz happens where the numbers are at near 0 dB afterwards. What is different is the odd pocket of good numbers, 2 dB and 4 dB, between 60 – 70 angles at 1.7 GHz. We can also see glimpse of those same good numbers at the very leftmost edge of the figure.

4.1.2 Wood

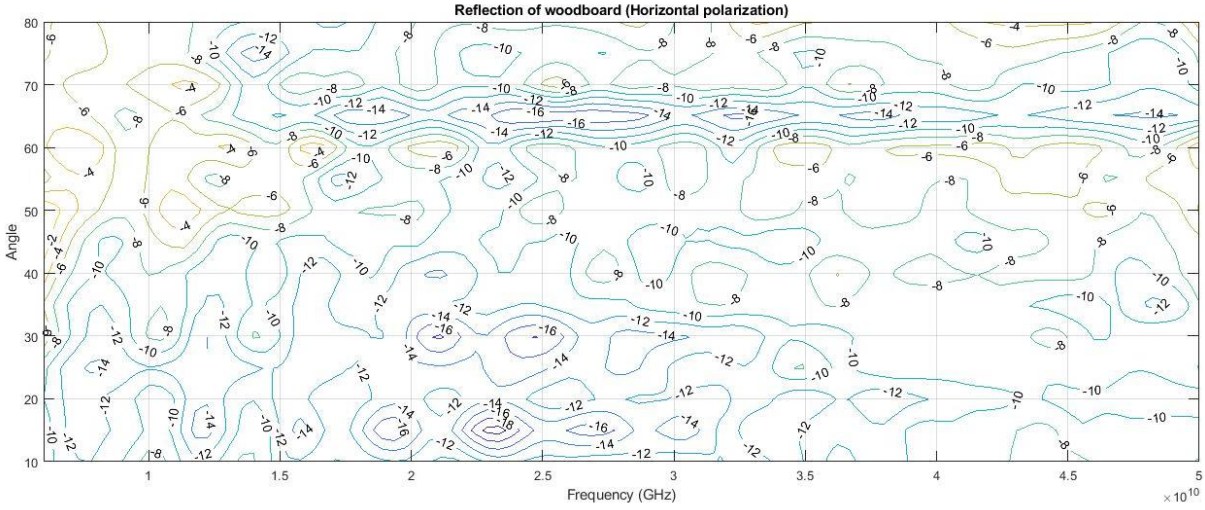

Figure 20. Horizontal polarization of wood board.

The horizontal polarization of wood has a period of bad reflections ranging from -8 dB to worst case -18 dB between 15 GHz and 50 GHz check that GHz is correctly spelled in all places in the angles of 60 – 70 degrees as shown in figure 20. There are also pocket of equally bad performance at 24 GHz in the low range of 10 – 20 degrees. Bright spots of -4 dB and -8 dB occur in the earlier frequencies at higher angles and the same at the higher end of the frequencies but less frequently.

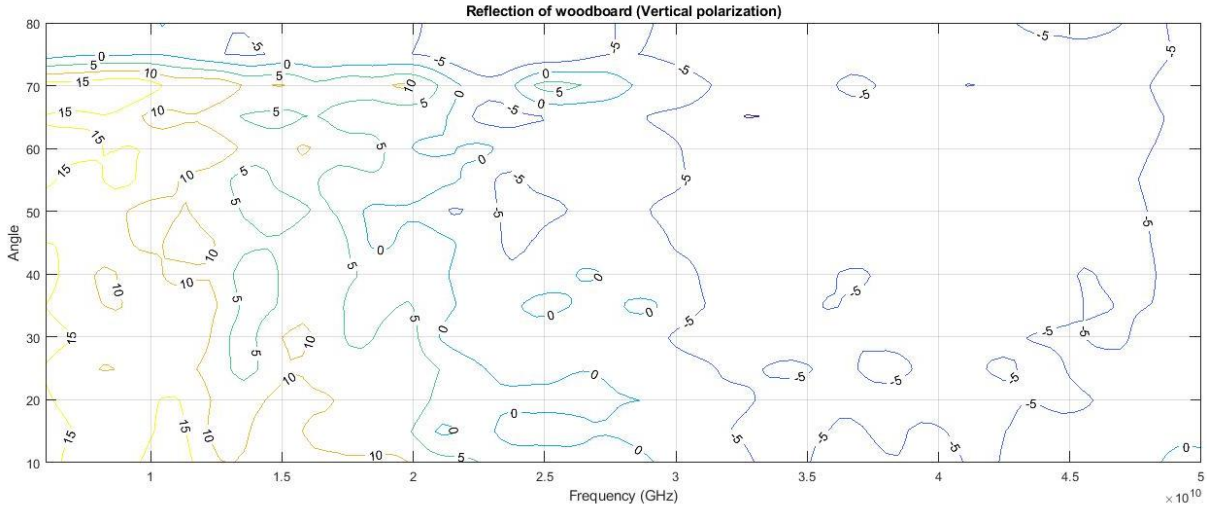

Figure 21. Vertical polarization of wood board.

The vertical polarization results of wood in figure 21 can be easily compared to the horizontal polarization. There is a gradual shift happening whereas the frequency increases, so too does the performance drop. From the beginning to 15 GHz is the best section with 10 dB, from there to 3 GHz the results are middling with 0 – 5 dB and the rest performing worst at -5 dB. The -5 dB results appears earlier than 3 GHz at 50- and 65-degree angles. Angles do not seem to affect much overall though. There is however a sharp drop-off in the 80 degrees which is surprising because it should offer the least amount of reflection loss.

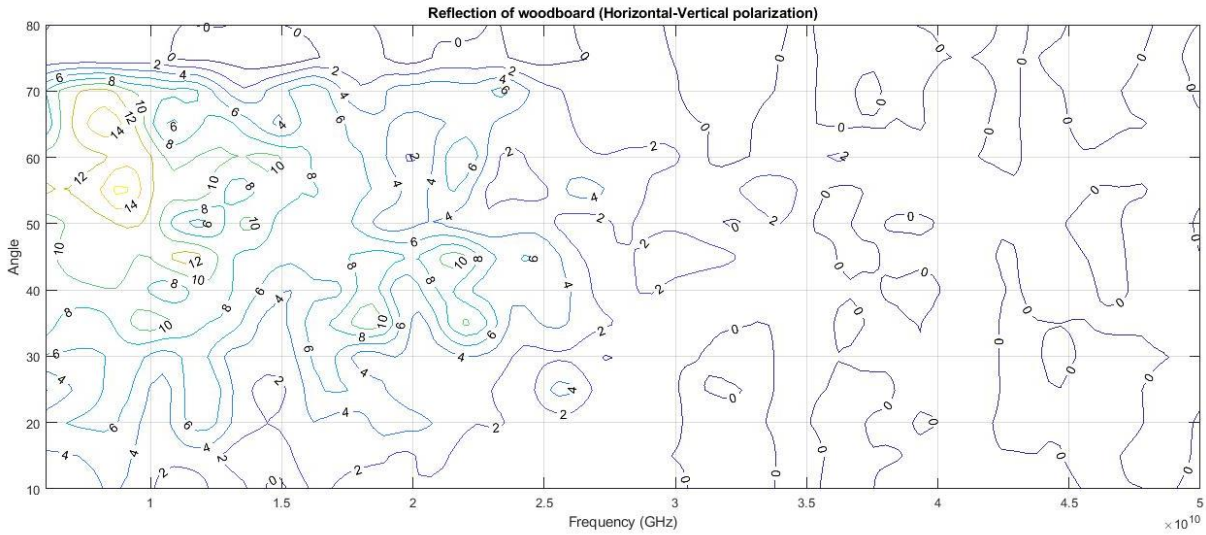

Figure 22. Horizontal-vertical polarization of wood.

The shift in horizontal-vertical polarization of wood is more instant as shown in figure 22. At 25 GHz, the results become more homogenous and middling. Briefly 4 dB and 2 dB before turning into 0 dB. This shift happens earlier for the smaller angles and to the highest angles too surprisingly. The 50 - 70 degree angles seem to be the sweet spot for reflections below 10 GHz. There the results are in double digits of 10 – 14 dB and trending towards zero with results between 8 – 4 dB outside that area.

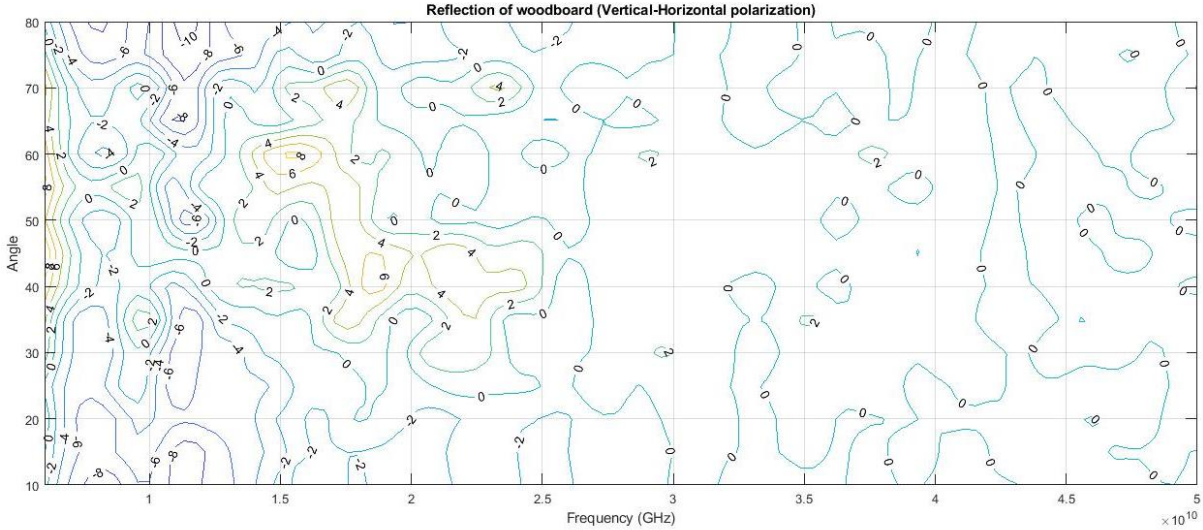

Figure 23. Vertical-horizontal reflection of wood.

The vertical-horizontal polarization results in figure 23 show some weirdness with less than stellar performance in the 10 GHz range. But it can be seen in the beginning and in 15 – 25 GHz range flashes of the positive numbers at minimum 2 dB and at maximum 8 dB. Both of those scenarios occur in the middle high angles and again, the extreme angles perform the worst dipping into the negative results between -2 dB and -10 dB. In the high frequencies, angles don't matter and everything looks the same near 0 dB result.

4.1.3 Plasterboard

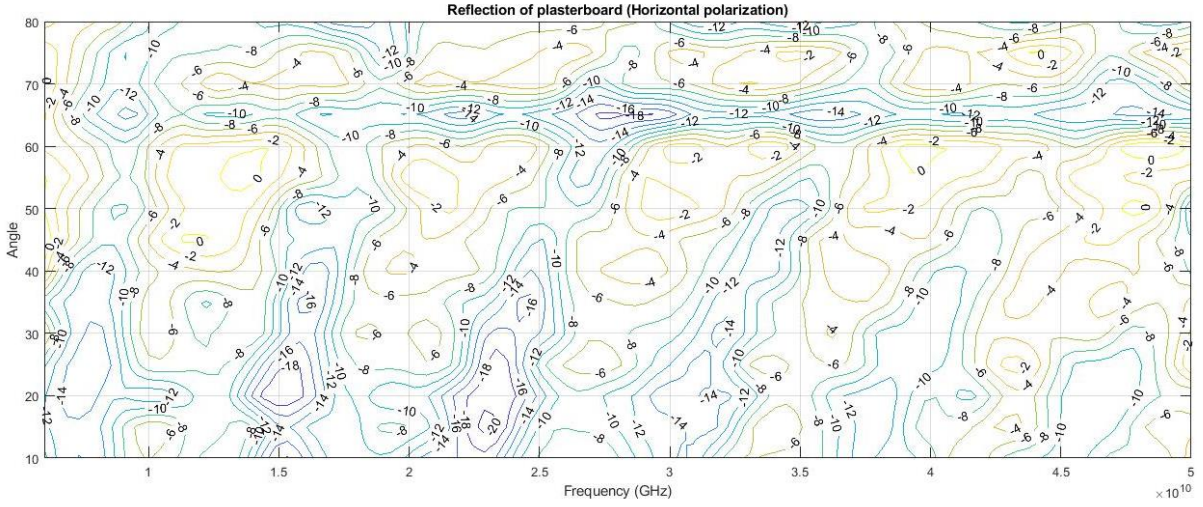

Figure 24. Horizontal polarization of plaster.

The horizontal polarization of plaster is very hard to read as shown in figure 24. There can be patterns observed if observed carefully. Between angles of 20 – 60 degrees and around 70 degrees, there seems to be alternating stripes of good to bad numbers. The best performing numbers are between -6 dB and 0 dB. The worse performing stripes are in double digit

territories with at worst -20 dB and at best -8 dB. While in the 70 – 80 degrees angles, it is just constant stream of similar double digit negative results mentioned previously. This behaviour happens in the low angles of 10 – 20 degrees but not as severely. Frequency does not seem to matter much here.

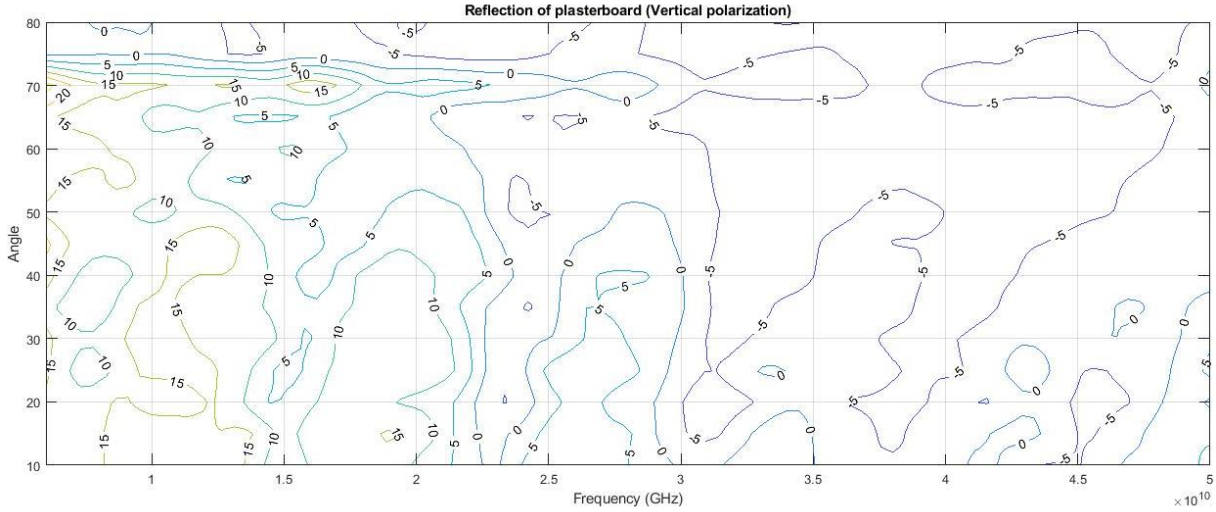

Figure 25. Vertical polarization of plaster.

Complete opposite of the horizontal polarization, the vertical results are much simpler to read from figure 25. The results are the best in the first half of the figure with numbers staying above 5 dB and reaching up to 20 dB and worse in the second half. There, the result changes between -5 dB and 0 dB. This is affected by frequency more then, where the higher frequency muffles reflections. As for angles, the only one showing any difference is around 70 degrees and higher where at the same frequencies of 6 – 2 GHz, the reflections are showing the same results as right half of the figure.

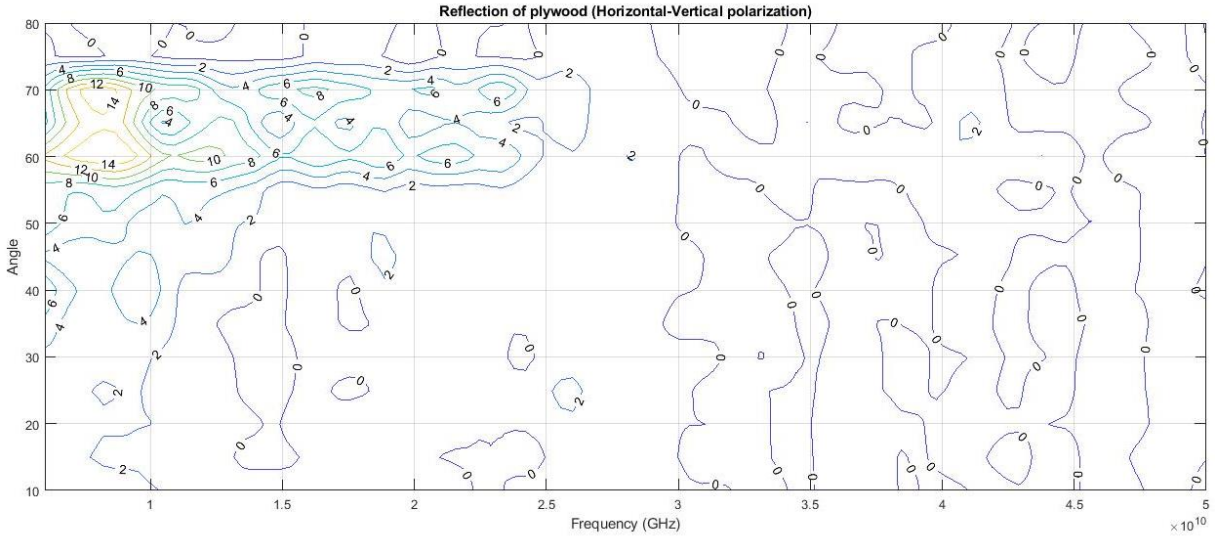

Figure 26. Horizontal-vertical reflection of plaster.

The horizontal vertical polarization of plaster seems to be as one would expect as shown in figure 26. The lower frequencies show better performance than the higher frequencies, staying

between 4 dB and 14 dB. Also, as you make the angle wider, the reflection can bounce off the material better and it shows in the better results. This too suffers from the degradation at 70 – 80 degrees angles though.

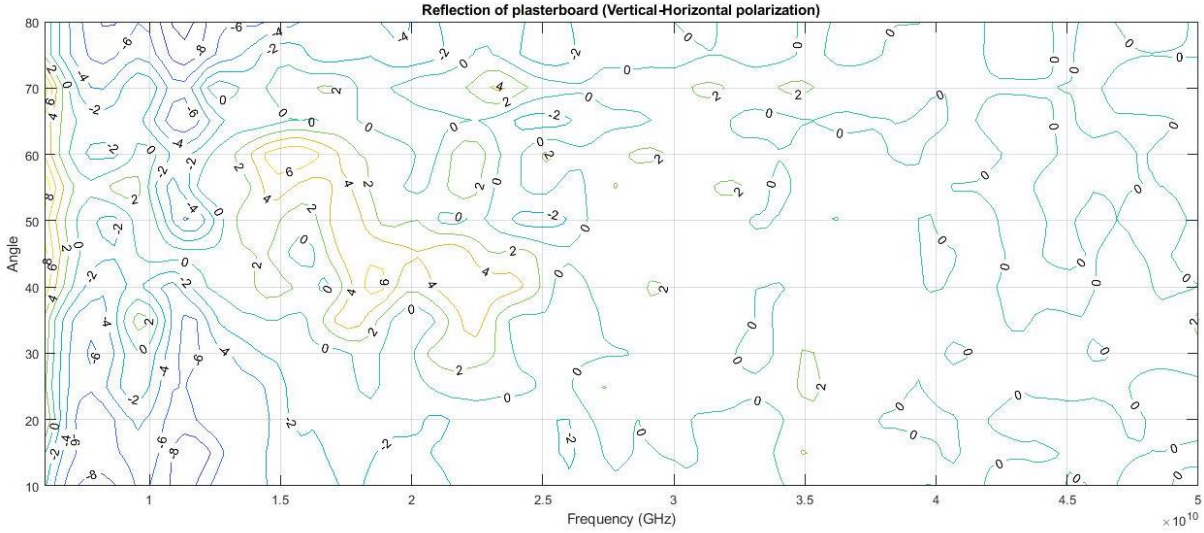

Figure 27. Vertical-horizontal polarization of plaster.

The vertical horizontal polarization of plaster seems to become less diverse after the middle frequency of 25 GHz in figure 27. Less differences happen and it is more of the same everywhere, either 0 dB or 2 dB. The beginning section has more frequent changes. They can alternate between -8 – 0 dB. Surprisingly the end section is still somewhat better than the first range of frequencies where the numbers can dip into negatives. The best section happens around 40 – 60 degrees and 15 – 25 GHz range where slightly positive results of 2 – 6 dB appear.

4.1.4 Ceramic Tile

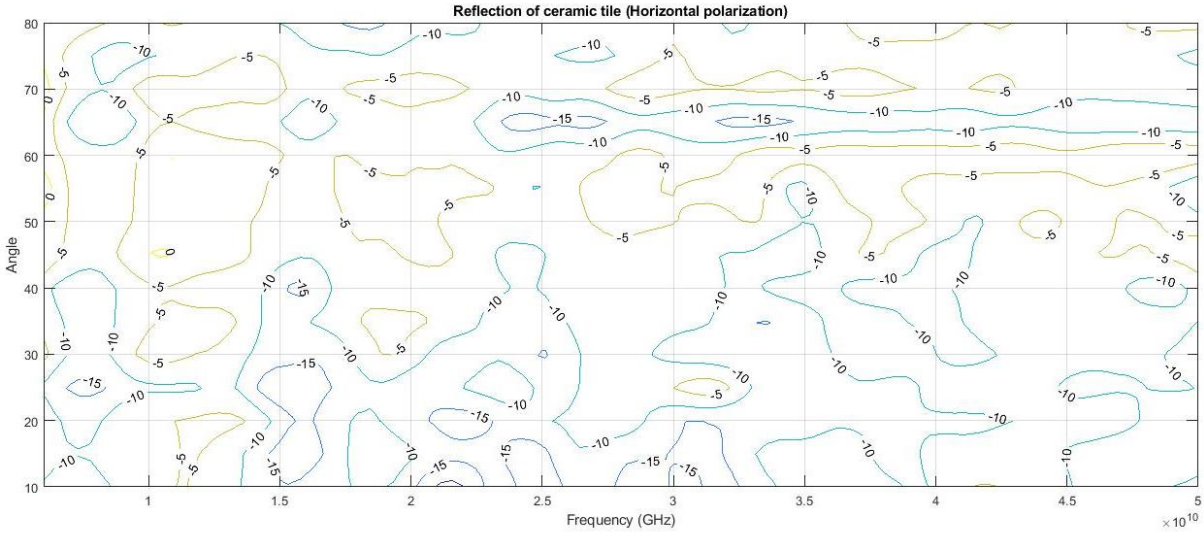

Figure 28. Horizontal polarization of ceramic tile.

The horizontal polarization of ceramic tile is surprisingly light in variations as shown in figure 28. There is a wide flow of -5 dB in 40 – 60 and 70 degree angles although both are becoming narrower the higher the frequency. The worst performance comes in the angles below 40 degrees exhibiting -15 dB and -10 dB at any frequency which makes sense with so sharp angles to reflect to and from. This also happens at angle of 65 degrees, initially rarely but then constant after 25 GHz.

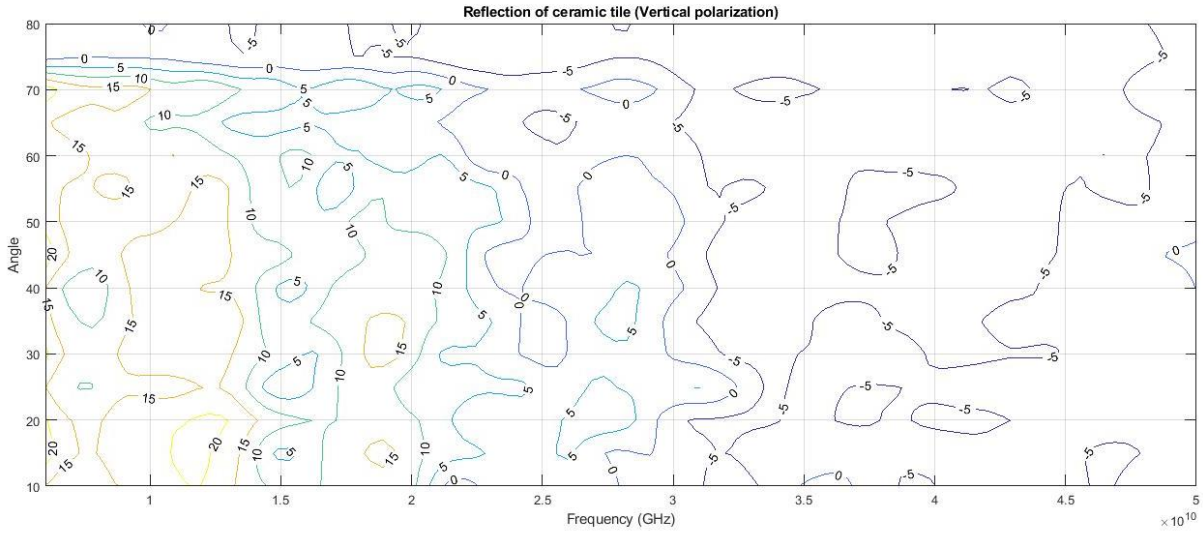

Figure 29. Vertical polarization of ceramic tile.

Ceramic tile's vertical polarization figure seems to show no apparent difference between the angles except at 80 degrees where it is -5 dB as worse as the later section of figure 29. The good performance of 5 – 15 dB is pretty apparent at even up to 20 GHz and it is still slightly good around 25 GHz before the numbers dip below zero.

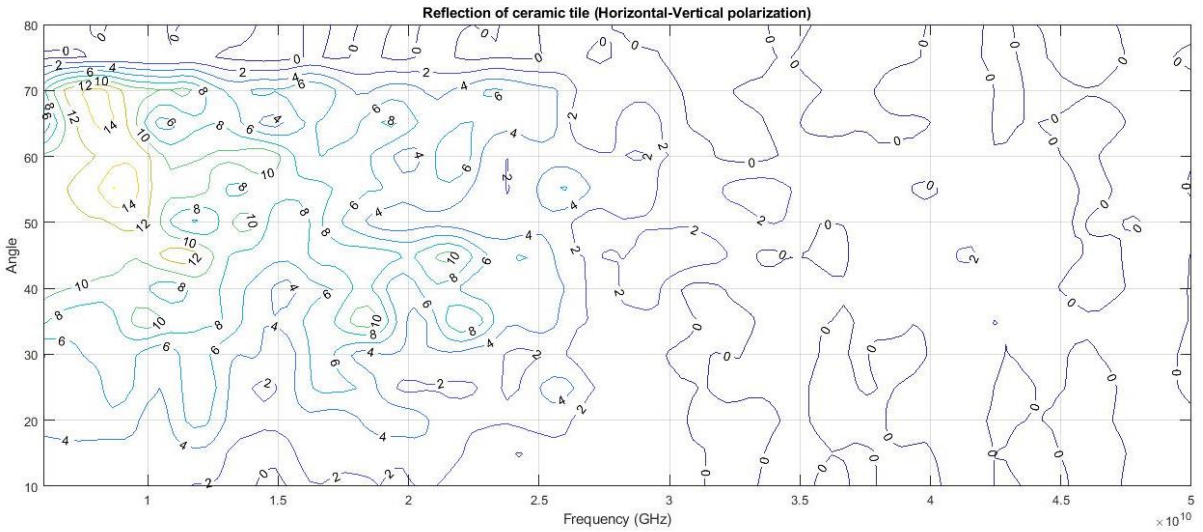

Figure 30. Horizontal-vertical polarization of ceramic tile.

The horizontal-vertical polarization of ceramic tile seems to be very similar in figure 30 compared to it's vertical polarization figure 29, but with more variance in the good results

section. There, the results can vary between the best of 10 – 14 dB and the rest 4 – 8 dB. These best results are in 70 – 50 degrees at 10 GHz and from there the numbers start a downward trend, the outer edges being 4 dB and 6 dB, the further they are before they reach 0 dB. The same block of high reflection loss values exists at the 80 degree angle.

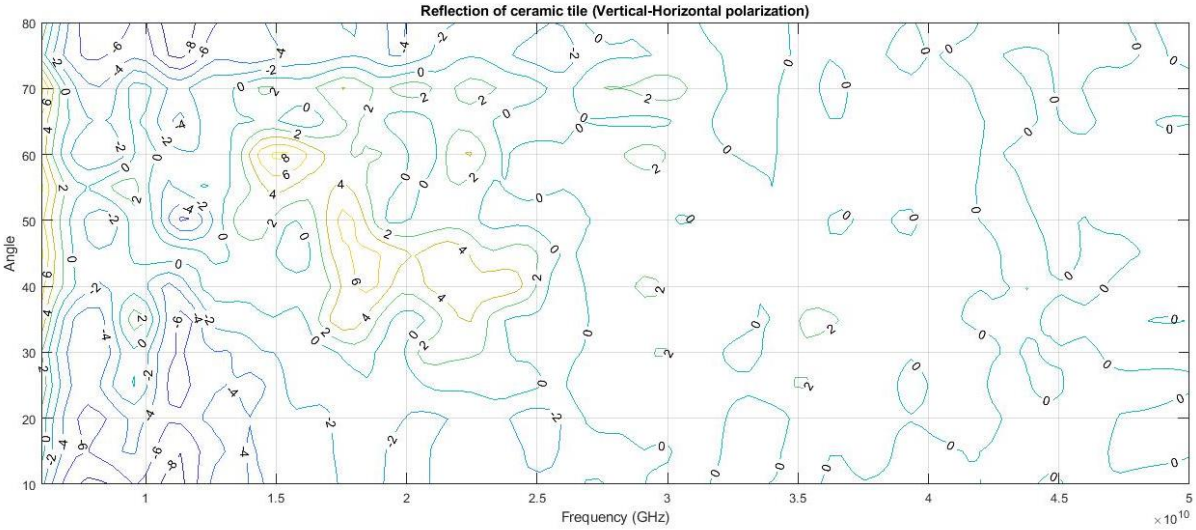

Figure 31. Vertical-horizontal polarization of ceramic tile.

The first section of the vertical-horizontal polarization of ceramic tile is very hard to make any observations from figure 31 about other than they are all bad drifting in -4 dB and -2 dB, with the worst results of -6 dB and -8 dB in the edge cases like 10 and 80 degrees. In the 15 – 25 GHz section, the reflections improve everywhere, even the worse performing angles, but especially in the 60 – 40 degrees range where they can be 2 – 8 dB. The higher frequencies look barren compared to the lower frequencies, staying at 0 dB.

4.1.5 Sidewall

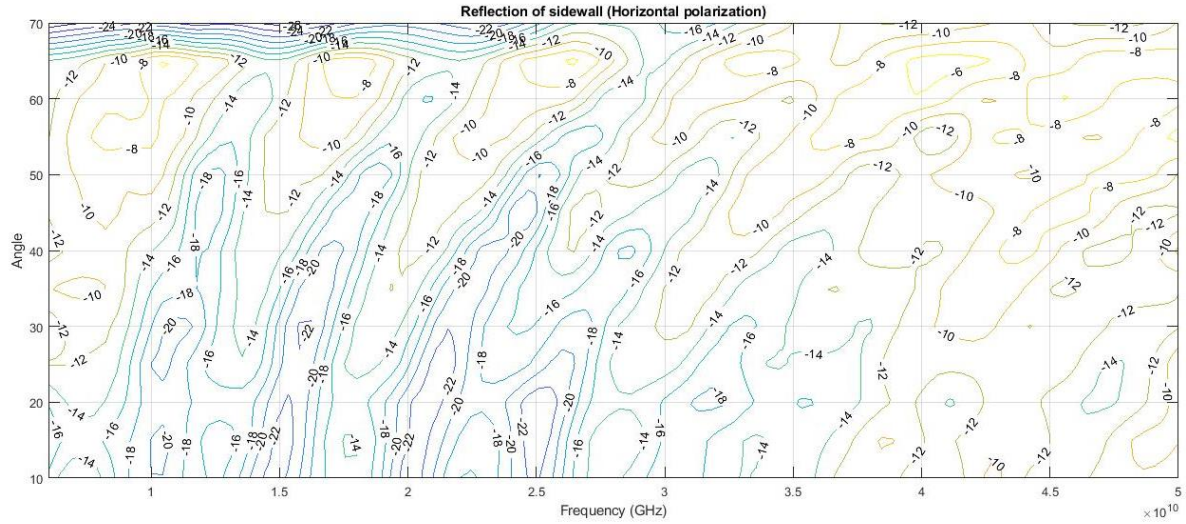

Figure 32. Horizontal reflection of sidewall.

The horizontal reflection of the sidewall sample is pretty distinct as shown in figure 32. Both frequency and angles seem to play a big part in affecting the results. The most muffled sections start from the beginning till around 35 GHz with results between -14 dB and -22 dB, but with some less bad spots between each two marks on the x-axis in the higher angles especially, results softening to -12 and -10 dB. This pattern makes it look like fingers on a hand. The wider the reflection angle, the better the results get, staying at -8 dB and -6 dB. This holds true for most of the graph except for the first half of frequencies at 70 degrees where they are some of the worst results at best -10 dB and at worst -24 dB.

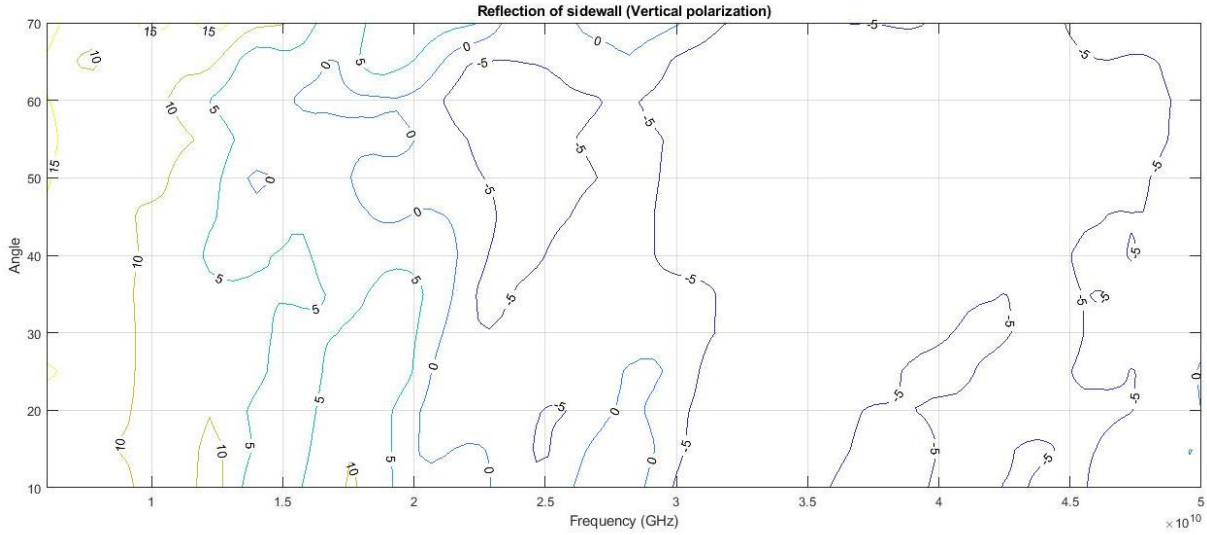

Figure 33. Vertical polarization of sidewall.

The vertical polarization of sidewall seems very straightforward in figure 33. It may be helped by the uniformity of the sample, but it doesn't explain the difference between the different polarizations. Perhaps the sample is made to flow into a certain direction less resistant

to vertical polarization. Angles don't play much part in this as the numbers are dictated by the frequency alone as it seems. The best numbers of 10 dB change to medium of 5 dB between 10 GHz and 15GHz and then to worst between 20 GHz and 25 GHz showing numbers between 0 dB and -5 dB.

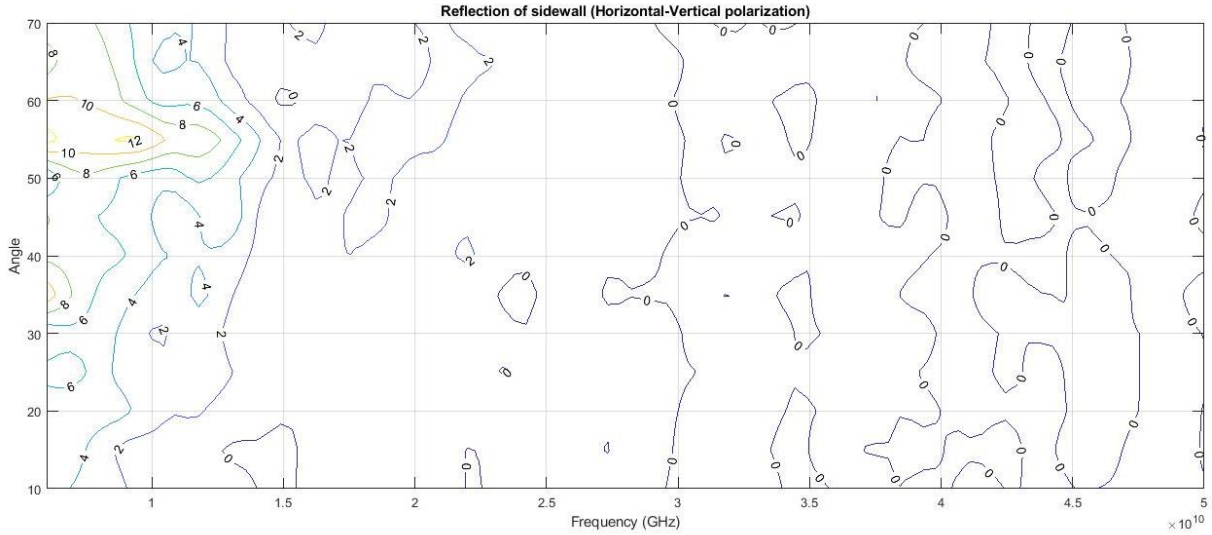

Figure 34. Horizontal-vertical reflection of sidewall.

The horizontal vertical polarization figure 34 has a large swath of almost emptiness in the middle. After that there is just the same number of zero repeating. The beginning part shows the best best performance at 50 - 60 degree angles. The wider angles have an increased space for good results in the frequency range.

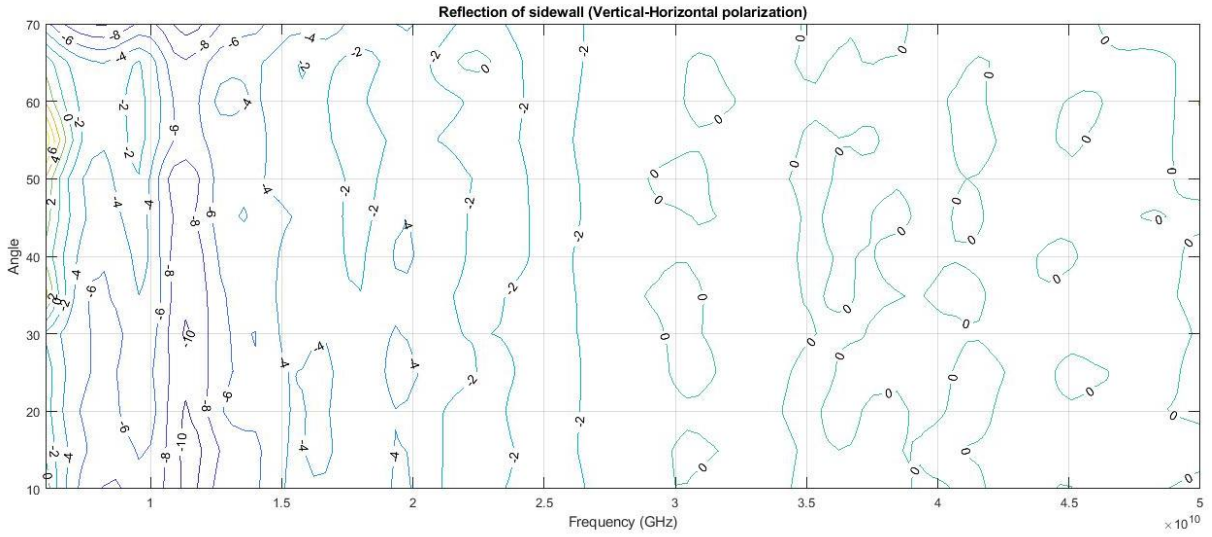

Figure 35. Vertical-horizontal reflection of sidewall.

The vertical-horizontal reflection figure 35 is organized nicely of vertically or over the measurement angles. The problem with it seems to be that it performs worse in the lower frequencies than higher. The higher angles help somewhat in reducing that bad performance, but it still does not look promising.

4.1.6 Conclusions

Similarities can be spotted with different material sample's reflections. For each one, the horizontal polarization figure is the most varied different from other polarization figures. It is also the worst performing of the four different polarization permutations. The two cross polarization figures seem to resemble the vertical polarization more than the horizontal one. Those three have this almost like vertical lines in their figures compared to horizontal polarization's more unique shapes. Whereas the horizontal figures can have different magnitudes depending on the angle and frequency, the other three looks to be more influenced by frequency alone than the angle. From midpoint of x-axis on, their results become homogenous where the angle doesn't matter much.

4.2 110 – 170 GHz Measurements

The 110 – 170 GHz measurements are done only in one polarization. Their plots are similar to each other, and some useful information can be gleamed. These measurements in general were smoother and less noise happened. This can be either from the antennas or the fewer cables used.

4.2.1 Plywood

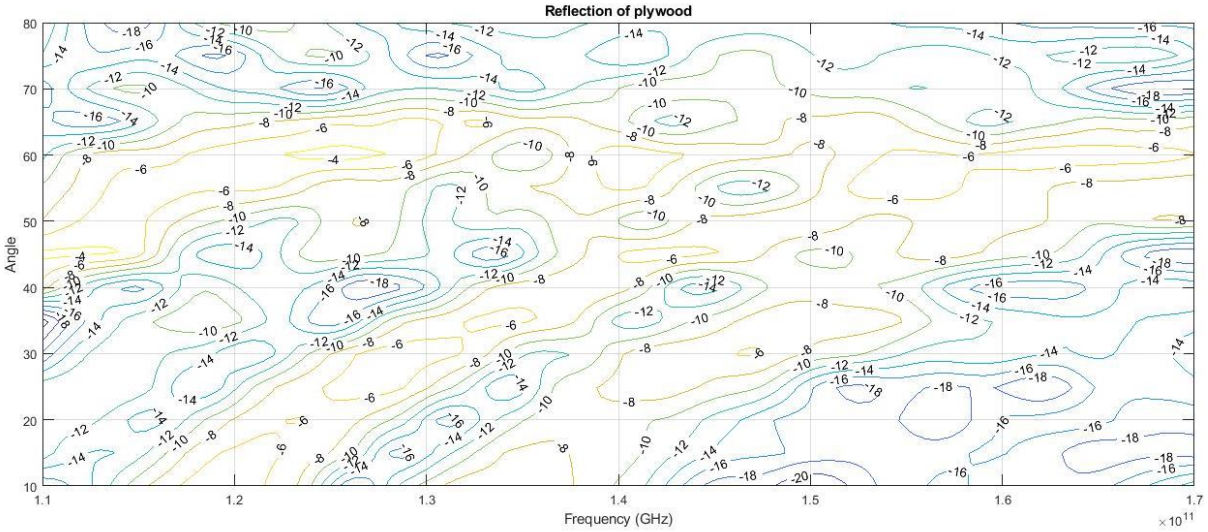

Figure 36. Reflection of plywood.

The reflection figure 36 of plasterboard is very messy but informative. From a glance, it looks three different streams of good numbers connecting into one at the end. In these streams, it varies between -8 dB to -4 dB. First of those is the one that starts and continues till the end which is occurring at about 50 – 60 degree angles. The second and third both start at lowest angles and drift upwards to combine to the first stream. The only thing different is their frequency, first one starts at 120 GHz and the second one at 135 GHz. Everywhere else it is ranging from -20 dB to -10 dB. This looks heavily affected by both frequency and angle.

4.2.2 Wood

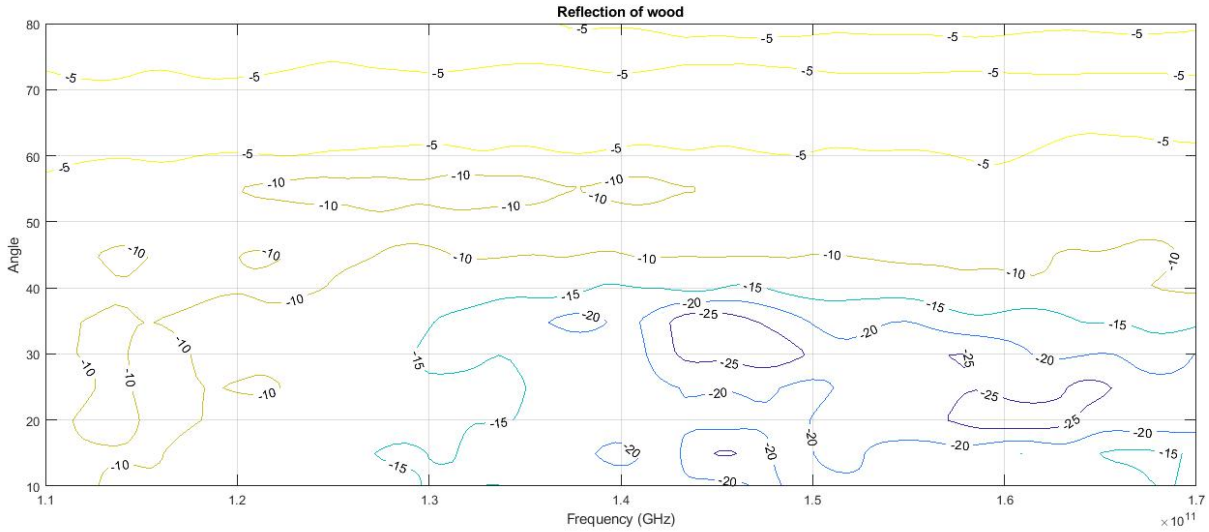

Figure 37. Reflection of wood.

The reflection of wood in these high frequencies shows almost no effect of frequency at wider angles in figure 37. From 60 degrees to 80 degrees, it is only performing at -5 dB. Between 40 degrees and 60 degrees, it is -10 dB and still not affected by frequency. Angles below 40 degrees, the higher frequency makes the reflections worsen noticeably. It is same as above with -10 dB until at around 130 GHz, it turns into -15 dB and going up to -25 dB. Above that angle though, the results are steadily the same. The figure is simple with little change except at the high frequency and low angle section part.

4.2.3 Plasterboard

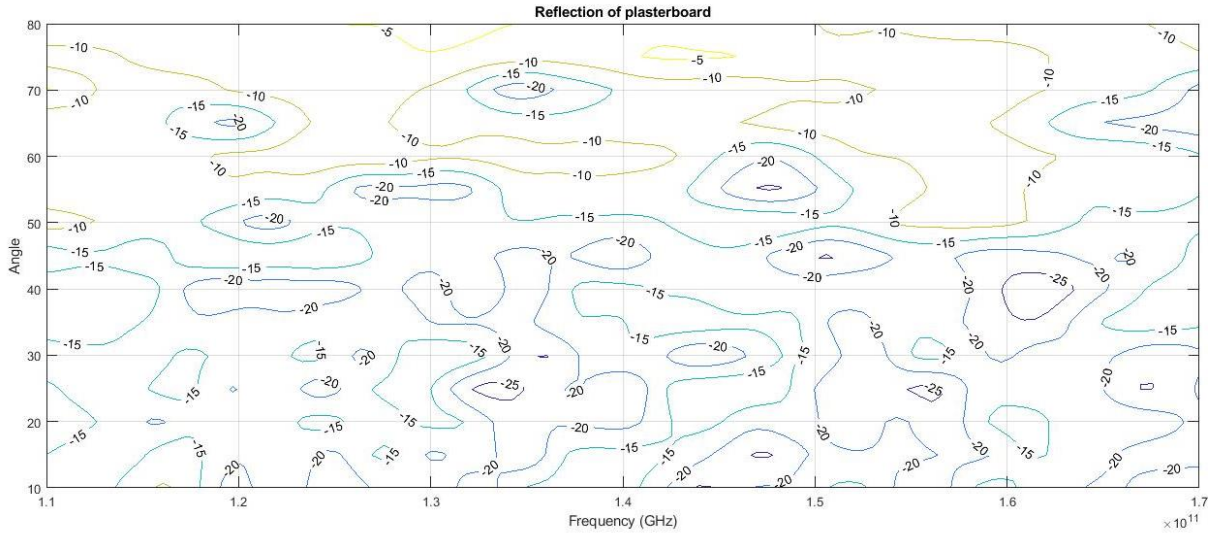

Figure 38. Reflection of plaster.

The changes in magnitude along the x-axis look so miniscule that frequency can be seen as not affecting much of the results in figure 38. More effective is the angle of measurements, with a high threshold to improve the result. Only at around 60 degrees do the magnitudes improve with results such as -10 dB and -5 dB and even then, there might happen worse performance of -20 dB and -15 dB at certain frequencies like 120GHz and 135GHz. The rest of the angles then perform the equally bad as the ones at those frequencies, just that they appear throughout. The bottom half of angles definitely are a bit random with some of the results, indicating again that frequency plays little part. At 170GHz. it does show the higher angles performing just as worse as the lower angles.

4.2.4 Ceramic Tile

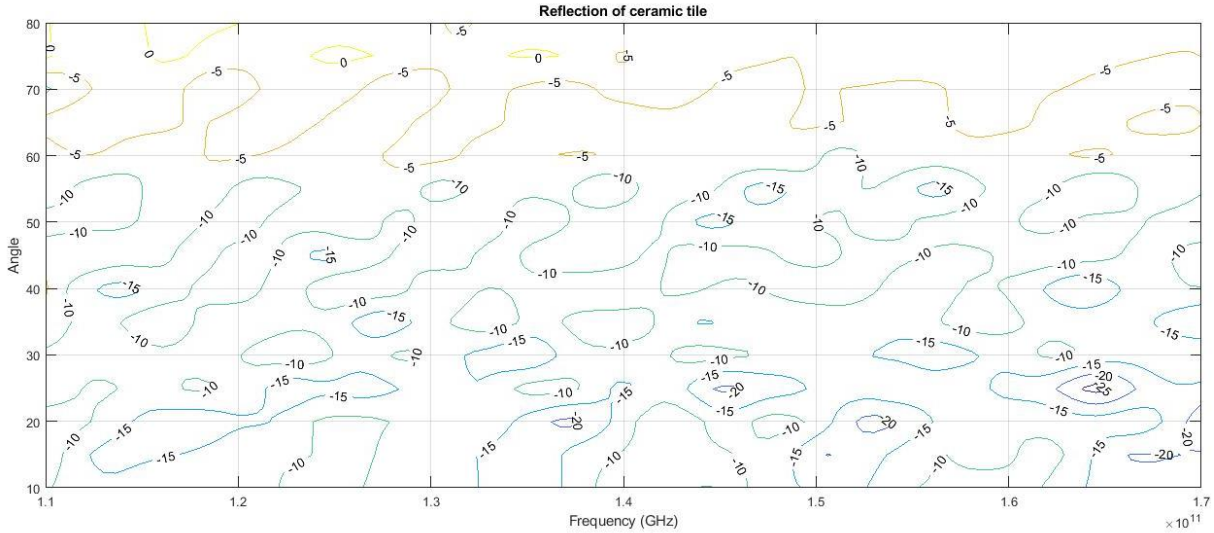

Figure 39. Reflection of ceramic tile.

The reflection of brick is consistent throughout in figure 39. Reflections of 0 dB at 80 degrees are the best and the reflections of -5dB at 60 – 70-degree angles are second best. The rest of the angles below are varying between -15 dB and -10 dB reflections with some -25 dB and -20 dB occurring at 25 degrees angle. It does not seem like the frequency dictates the reflections almost at all.

4.2.5 Sidewall

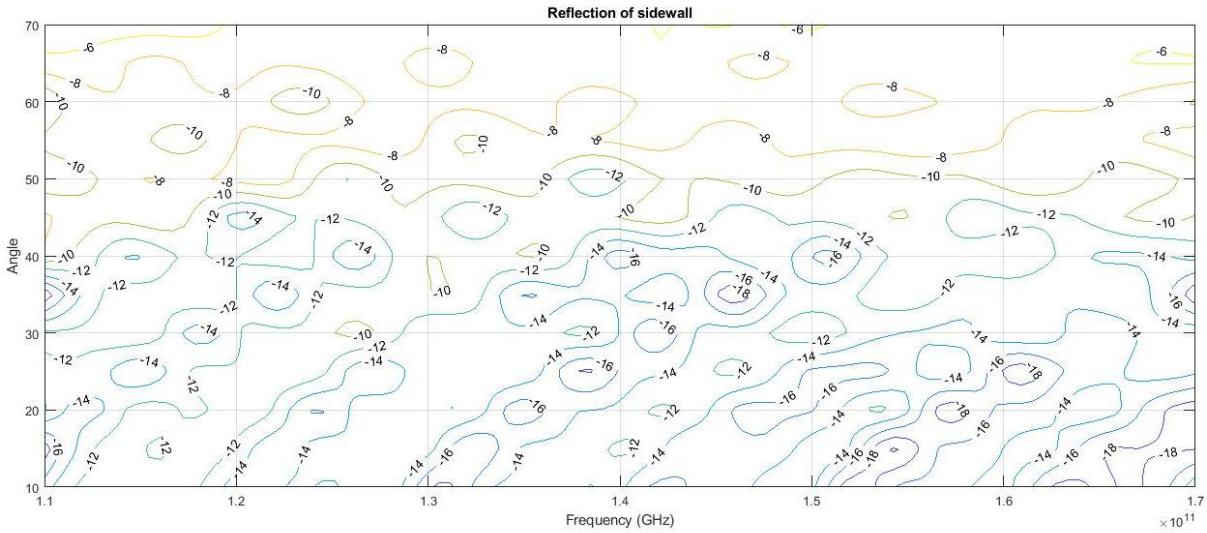

Figure 40. Reflection of sidewall.

The sidewall material is the most uniform looking of the samples, and it reflects in the results of figure 40. The angle affects the reflections most with frequency slightly worsening the results in the second half of the figure. Below 40 degrees, results between -18 dB and -12 dB occur and at 50 degrees, it is more constant of -10 dB. Any higher angles predominantly perform at -8 dB with some flashes of -6 dB.

4.2.6 Conclusions

The 110 – 170 GHz measurements show a clear picture of how much the angle does affect at such high frequencies. The best performing angle is repeatedly the highest measured which is the 80 degrees or 70 degrees in case of the sidewall. In the lower angles, the numbers are the worst all over the place so it cannot be said which angle is the worst performing. Just that, the wider you make the reflection angle, the less it matters. As for frequency, most of the samples performed noticeably worse at the higher end of the x-axis. Curiously, this frequency effect affected only the lower angle results. At higher angles, the performance did not change much going from the beginning frequency to end.

5 DISCUSSION

The reflection measurement results are a mixture of as expected and some surprises. The 6 to 50 GHz measurements revealed how much the horizontal and vertical polarizations can differ from each other. The horizontal co-polarization produced very informative figures with a lot of data points. Vertical polarization figures were more one note and light on detail. Nevertheless, the latter did show better results in almost every spot of the coordinate. In the higher frequencies, the numbers started to shift to being zero in almost every case. The cross-polarization figures seemed to take after the vertical polarization more than the horizontal figures. Both cross-polarizations had vertical lines from left to right and quickly shifted downwards by the middle. They still performed better than horizontal polarization on its own. Angle of incident seemed to affect very little with just the extremes being able to change the numbers from the norm. Surprisingly both the lowest and the maximum angles were worst performing.

This is in complete contrast to the 110 to 170 GHz measurements where the frequency did not change anything, and the angle of incident commanded the results. The lower angles performed the worst and depending on the material, around 40- or 50-degrees reflections started to improve. For each material in the higher frequency set, the widest angle performed best since it gives the sharpest bounce off the material.

During the thesis work, much effort was spent to design the measurement system. There were examples of similar measurements, but they were found to be not suitable or possible for this work. The measurements went as best as they could with the constraints given overall. Challenges discovered and ways to improve the measurement system in future works are discussed in the following chapter.

Many of the challenges in these measurements came from the lack of proper equipment. The 6-50GHz measurements needed a specific set of coaxial cables of which only couple short length ones were available. As a compromise the three short coaxial cables were connected to each other to extend the length and then calibrate the antennas. Even with this, the cables had to be pushed to their limit and all that coaxial bending is not ideal.

The second topic is the material selection. At first, the measurements were thought to take place in and around the University of Oulu against different wall materials. This proved hard to carry with the low mobility of the VNAs. Eventually, it was settled on that the measurements will be done in the EMC lab and thus, material samples had to be self-sourced. This led to not quite ideal samples with imperfections, but it does differentiate the work from others. The materials were small enough that the antennas had to be made sure to point directly at them with the help of a laser.

The measurement results still contained much noise inside the EMC laboratory, particularly in the dual-polarized measurements, that would require further investigations. The measurement noise increased at the higher frequency of the 6 to 50 GHz measurements. Applying the smoothing algorithm averaged it, but it might have made data too uniform and that is why there is a lot of similarities at the higher frequencies of first measurement set.

6 SUMMARY

This work aimed at discovering how the degree of angles combined with such high frequencies affected the signal strength of the reflected signal. The measurements were separated into two different frequency bands. The lower frequency of the two, 6 to 50 GHz, were measured with dual polarized antennas for further study. The 110 to 170 GHz measurements used a frequency extender. The measurements were done in an EMC laboratory and constructing the setup took some time. The measurements themselves were simple but laborious since the antennas had to be shifted by five degrees to the next angle and the absorption block to the best places to avoid straight communication between the antennas by hand. LOS measurement was done to reduce the distance loss from the results afterwards.

Material samples consisted of five different wall materials common in the real world: plywood, wood of a cutting board, ceramic tile, plaster and sidewall from an office environment. The samples were not the largest, but big enough for signals to bounce from. A half circle was used to angle the antennas in line with the desired degrees. The antennas were ensured to be placed in a distance higher than the minimum required for far field results. They were held in place quite high above the ground in case of rogue signals bouncing from the ground.

The results were stored on the VNA either as s4p or csv files and transported with a memory stick. Matlab was the program of choice to represent the data into palatable figures. With such large amount of data, each simulation took tens of minutes. It was concluded from the results that frequency was the dominant force in the 6 to 50 GHz measurements while it did not affect almost anything in the 110 to 170 GHz frequency band. Compared to angle which played a minimal part in all the polarizations of 6 to 50 GHz frequency band although it did affect in the minimum and maximum angles, but was the major, if not the only, driving force in the 110 to 170 GHz measurements.

7 REFERENCES

[1] A. Aragón-Zavala, Indoor Wireless Communications: From Theory to Implementation, Hoboken, NJ: John Wiley & Sons, 2017.

[2] C. G. Christodoulou ja P. Wahid, Fundamentals of antennas: concepts and applications, Bellingham, WA: SPIE, 2001.

[3] W. L. Stutzman ja G. A. Thiele, Antenna Theory and Design, 3rd Edition, John Wiley & Sons, 2012.

[4] L. V. Blake ja M. W. Long, Antennas: Fundamentals, Design, Measurement, Raleigh, NC: Scitech Publishing, 2009.

[5] Antenna Theory, "Field Regions," [Online]. Available: https://www.antenna-theory.com/basics/fieldRegions.php. [Accessed 16 June 2022].

[6] C. A. Balanis, Antenna Theory: Analysis and Design, Hoboken, NJ: John Wiley & Sons, 2016.

[7] T. S. Rappaport, Wireless Communications: Principles and Practice, Prentice Hall, 2002.

[8] W. L. Stutzman, Polarization in Electromagnetic Systems, Norwood, MA: Artech House, 2018.

[9] National Instruments, "Introduction to Network Analyzer Measurements Fundamentals and Background," [Online]. Available: http://download.ni.com/evaluation/rf/Introduction_to_Network_Analyzer_Measurements.pdf. [Accessed 16 June 2020].

[10] F. Caspers, "RF engineering basic concepts: S-parameters," in *CAS - CERN Accelerator School: RF for Accelerators*, Ebeltoft, Denmark, 2010.

[11] Rohde & Schwarz, Fundamentals of Vector Network Analysis, Columbia, MD: Rohde & Schwarz USA.

[12] N. Shoaib, Vector Network Analyzer (VNA) Measurements and Uncertainty Assessment, Cham, Switzerland: Springer Internatiol Publishing, 2017.

[13] bsw TestSystems & Consulting, "Frequency Expansion Modules up to 1.5THz for Network Analyzers," [Online]. Available: https://www.bsw-ag.com/en/instruments-frequency-extenders.html. [Accessed 16 June 2022].

[14] Virginia Diodes, Inc, *VNA Extension Modules Operational Manual,* Charlottesville, VA, 2020.

[15] R. Sharma and A. C. Suthar, "Design and Analysis of Pyramidal Horn Antenna as Plane Wave Source for Anechoic Chamber," Journal of Advances and Scholarly Researches in Allied Education, vol. 16, no. 4, March 2019.

[16] U. Barapatre, S. Panchal, J. M. Rathod, P. H. Panchal and K. Parikh, "Design and Analysis of Quad Ridged Horn Antenna for High Gain Application," Journal of Physics: Conference Series, vol. 1706, no. 1, 2020.

[17] R. C. Johnson, Antenna Engineering Handbook 3rd ED, New York, NY: McGraw Hill, 1993.

[18] Pasternack, WR-6 Waveguide Standard Gain Horn Antenna Operating from 110 GHz to 170 GHz with a Nominal 25 dBi Gain with UG-387/U-Mod Round Cover Flange Specifications, Irvine, CA, 2019.

[19] A-INFO, LB-SJ-50500 5.0 - 50.0GHz Dual Polarization Horn Antenna.

[20] RF Spin, *QRH67E Datasheet,* Prague, Czech Republic, 07-2021.